Telmo Gabriel Simões Fernandes

Time-Interleaved BWB-OFDM with Iterative FDE

Dissertação submetida para a satisfação parcial dos requisitos do grau de Mestre em Engenharia Electrotécnica e de Computadores na especialidade de Telecomunicações

Setembro 2015

· U C ·

UNIVERSIDADE DE COIMBRA

Time-Interleaved BWB-OFDM with Iterative FDE

Telmo Gabriel Simões Fernandes

Dissertação para obtenção do Grau de Mestre em

Engenharia Electrotécnica e de Computadores

Orientador:	Doutor Marco Alexandre Cravo Gomes
Co-Orientador:	Doutor Vítor Manuel Mendes da Silva

Júri

Presidente:	Doutor Mário Gonçalo Mestre Veríssimo Silveirinha
Orientador:	Doutor Marco Alexandre Cravo Gomes
Vogal:	Doutora Maria do Carmo Raposo de Medeiros

Setembro de 2015

When I was 5 years old, my mother always told me that happiness was the key to life. When I went to school, they asked me what I wanted to be when I grew up. I wrote down 'happy'. They told me I didn't understand the assignment, and I told them they didn't understand life.

- John Lennon

I have not failed. I've just found 10,000 ways that won't work.

- Nikola Tesla

Watch a sunrise at least once a day.

- Phil Dunphy

Agradecimentos

Gostaria de começar por agradecer ao professor Marco Gomes pela oportunidade de participar neste projecto, pela sua capacidade de trabalho, motivação, amizade, experiência e pelo privilégio da sua orientação. Ao professor Vítor Silva pelo seu acompanhamento, pela sua disponibilidade constante e pela sua capacidade de revolver problemas. Ao professor Rui Dinis por me abraçar neste projecto e pelo seu apoio.

Ao Instituto de Telecomunicaçõess por todos os meios disponibilizados e pelo ambiente de trabalho descontraído e profissional que se vive, e à Fundação para a Ciência e Tecnologia, por ter financiado em parte este trabalho.

Aos meus colegas de curso por todas as experiências vividas durante o meu percurso académico, com um agradecimento especial aos eternos Ohms de Negro.

Sinto uma eterna gratidão aos meus pais e à minha irmã pelo seu esforço e dedicação, pela imcomparável disponibilidade e vontade de me ajudarem sempre a atingir os meus objectivos e por crescer com eles todos os dias.

A todos os meus amigos que me acompanharam e apoiaram ao longo desta importante etapa,

Muito Obrigado.

Abstract

The remarkable progress in wireless communication services achieved over the past decade led to a demand in high data rate applications, spectral efficiency and flexibility requirements. The new recently proposed Block-Windowed Burst OFDM (BWB-OFDM) transceiver scheme proved to be a reliable alternative scheme to face these current demands. This multicarrier technique employs smoother, non-rectangular windows, allowing a power spectral density (PSD) similar to the filtered OFDM approach but instead of using a cyclic prefix to each symbol it assembles a set of symbols and only then appends a sole zero-padding (ZP) guard interval to accommodate the multipath channel's propagation delay, which means better overall power and spectral efficiencies. Moreover, this scheme allows a commitment between better signal spectrum confinement and a higher transmission rate. However, the bit-error rate gain relatively to conventional OFDM schemes is low and its performance is far from the theoretical limit (matched filter bound). The main goal of this work is to achieve BER performances as close to the theoretical limit as possible keeping the benefits achieved by the BWB-OFDM scheme. The superior performances achieved by nonlinear iterative equalizers applied to SC-FDE schemes motivate the implementation of the popular IB-DFE technique in the BWB-OFDM architecture. Nevertheless, the deep fading wireless channel is an obstacle to this accomplishment. By stressing the drawback of the BWB-OFDM scheme over these channels, a new transceiver scheme, built on the BWB-OFDM architecture, is proposed. The time-interleaved BWB-OFDM employs a time-interleaver on the transmitted time block aiming to preserve the data severely corrupted by the channel's deep fading issue. The results of this new proposal are presented with a receiver that employs the IB-DFE technique, allowing substantial gains relatively to the BWB-OFDM scheme and at the same time pretty close to the theoretical limit.

Keywords

Iterative Block Decision Feedback Equalization (IB-DFE), Block-Windowed Burst OFDM (BWB-OFDM), Time-Interleaver, Deep Fading

Resumo

O notável progresso nos serviços de comunicação *wireless* verificado na última década levou a uma procura de aplicações com altas taxas de transmissão, maior eficiência espectral e melhores condições de flexibilidade. O esquema de trasmissão intitulado Block-Windowed Burst OFDM, recentemente proposto, demonstrou ser um esquema alternativo fiável para satisfazer essa procura. Esta técnica multiportadora emprega janelas no transmissor com transições mais suaves, permitindo obter uma densidade espectral de potência (PSD) semelhante à obtida pelo *filtered*-OFDM, no entanto, em vez de adicionar um prefixo cíclico a cada símbolo, este concatena um conjunto de símbolos e só depois adiciona um intervalo de guarda *zero-padding* (ZP) de forma a acomodar o efeito dispersivo do canal, resultando, em geral, numa melhor eficiência espectral e energética. Além disso, este esquema permite um compromisso entre taxas de transmissão efectivas mais elevadas e um maior confinamento espectral. No entanto, o ganho em termos de *bit-error rate*, relativamente a esquemas OFDM convencionais é baixo e o seu desempenho ainda está aquém do limite teórico (*matched filter bound*). O objectivo principal deste trabalho é atingir desempenhos perto do limite teórico, mantendo os benefícios alcançados pelo esquema BWB-OFDM. O desempenho superior alcançado por equalizadores não-lineares iterativos aplicados a esquemas SC-FDE motivam a implementação da técnica popular IB-DFE, no esquema BWB-OFDM. No entanto, um canal com condições severamente hostis, nomeadamente, desvanescimentos profundos, apresenta um entrave a esta implementação. Ao destacar a desvantagem do esquema BWB-OFDM perante este tipo de canais, um novo esquema, baseado na arquitectura BWB-OFDM, é proposto. O *time-interleaved* BWB-OFDM emprega uma intercalação no domínio do tempo ao bloco a transmitir para preservar dados que serão corrompidos devido ao efeito de desvanescimento profundo. Os resultados desta nova proposta são apresentados com um receptor que aplica a técnica IB-DFE, alcançando ganhos substanciais em relação ao esquema BWB-OFDM e, ao mesmo tempo, alcançando um desempenho muito próximo do limite teórico.

Palavras-Chave

Iterative Block Decision Feedback Equalization (IB-DFE), *Block-Windowed Burst OFDM* (BWB-OFDM), *Time-Interleaver*, Desvanescimento Profundo

Contents

List of Figures

List of Acronyms

ACI	adjacent channel interference
AWGN	additive white gaussian noise
BER	bit error rate
BWB-OFDM	block-windowed burst orthogonal frequency division multiplexing
CP	cyclic prefix
CS	cyclic sufix
DFT	discrete fourier transform
FD	frequency domain
FDE	frequency domain equalization
FFT	fast fourier transform
IB-DFE	iterative block decision feedback equalization
IDFT	inverse discrete fourier transform
IFFT	inverse fast fourier transform
ICI	inter-carrier interference
ISI	intersymbol interference
LDPC	low-density parity-check
LLR	log-likelihood ratio
MC	multi-carrier
MFB	matched filter bound

MMSE	minimum mean square error
MSE	mean squared error
OBO	output back-off
OFDM	orthogonal frequency division multiplexing
PA	power amplifier
PAPR	peak-to-average power ratio
PSD	power density spectrum
QAM	quadrature amplitude modulation
QPSK	quadrature phase shift keying
SC	single carrier
SC-FDE	single-carrier frequency domain equalization
SINR	signal-to-interference plus noise ratio
SNR	signal-to-noise ratio
SRRC	square-root raised cosine
ZF	zero forcing
ZP	zero-padding

1

Introduction

The next generation of mobile communications is a hot topic between researchers. Such focus is due to the tremendous growth of mobile phone users and the remarkable progress made which allowed wireless communication services to become a reality.

High data rate is desired in many applications, thus demanding the development of power and bandwidth air interface schemes. One obstacle to that development lies in the dispersive nature of the wireless channel. The dispersion phenomena arises from the several paths that the transmitted signal may follow during a transmission between either static or mobile users, thus reaching the receiver with different time delays causing intersymbol interference (ISI) and fading. To combat time-dispersive fading channels, multi-carrier systems arose with the first proposal to use parallel data transmission published around 1967 [4].

Meanwhile, Orthogonal Frequency Division Multiplexing (OFDM) has become the favorite multicarrier modulation technology for wireless communication systems [4]. Such preference is justified by its low computational complexity, since it takes advantage of the fast discrete-time Fourier transform (DFT) algorithms. The OFDM principle is to divide the channel into narrow band flat fading sub-channels with considerable spectral efficiency attained by overlapping the sub-channels with possible inter-carrier interference (ICI) avoided by the orthogonality condition. Also, a cyclic extension is appended to each OFDM symbol accommodating the dispersive channel effect, thus avoiding usual ISI. The cyclic extension is discarded at the receiver which allows frequency-domain equalization (FDE) with just a multiplier factor at each sub-carrier [5] [6]. However, OFDM has a set of drawbacks that motivated the search for an alternative scheme.

The main disadvantages concerning OFDM techniques are its high out-of-band signal energy since the applied rectangular pulse has a very large bandwidth due to the high sidelobe level and its high peak-to-average power ratio (PAPR). This last one is of utmost importance since a power amplifier (PA) is one of the most expensive components in a communication system [7] [8]. To tackle those issues the recent Block-Windowed Burst OFDM (BWB-OFDM) transceiver scheme was proposed [3] [2]. This scheme aims to reach a commitment between higher data rate and spectrum confinement and reduced PAPR levels due to its employment of smoother, non-rectangular windows and the avoidance of cyclic prefix (CP), providing better overall power and spectral efficiency.

1.1 Motivation and Objectives

Although, the overall power and spectral efficiency of the BWB-OFDM technique is better than filtered and conventional OFDM schemes, the receiver lacks a equalizer capable of achieving a performance close to theoretical limit (matched filter bound). Recently,

it has been shown that Single Carrier Frequency Domain Equalization (SC-FDE) schemes have an overall performance advantage over OFDM when employing the Iterative-Block Decision Feedback Equalization (IB-DFE), a nonlinear equalizer that can outperform linear equalizers [9]. However, the mentioned iterative FDE technique is only conceived for SC modulation but, in the new BWB-OFDM transceiver scheme, the received signal can be regarded as of an SC-FDE type which prompts the employment of the IB-DFE with the BWB-OFDM technique.

As so, the purpose of the investigation developed on the course of this dissertation is to propose and develop a new transceiver architecture built on the BWB-OFDM technique exploring the benefits of the IB-DFE technique with the aim to achieve performances as close to matched filter bound (MFB) as possible.

The development of the new transceiver scheme, designated by *time-interleaved* BWB-OFDM was carried out under the project GLANCES (Generalized Linear Amplification with Nonlinear Components for Power and Spectral Efficient Broadband Wireless Systems, supported by Instituto de Telecomunicações - IT). This thesis work provided a paper under development.

1.2 Dissertation Outline

This thesis is organized in five chapters. This chapter introduces the topic of the thesis, the motives that led to this particular investigation and also stresses the main goals proposed to achieve. Chapter 2 introduces the concept of OFDM, exposing its advantages and disadvantages, with an extensive and detailed system analysis. Later in the same chapter it introduces the recently proposed BWB-OFDM scheme stressing the overall improvements towards typical CP-OFDM schemes. Chapter 3 describes the basic structure of an IB-DFE receiver with emphasis on mathematical formulation. On chapter 4 the performance of the BWB-OFDM technique combined with an IB-DFE receiver is evaluated. It is followed by the analysis of the performance results which leads to the proposal of the appliance of a time-interleaver to the transmitted BWB-OFDM block. This proposal induces a new architecture scheme which is presented. The performance of the new time-interleaved BWB-OFDM scheme is compared to the BWB-OFDM scheme employing MMSE and over several iterations performed employing an IB-DFE and a turbo IB-DFE. It ends with a PAPR level evaluation. Chapter 5 is concerned with the conclusions drawn from this thesis and presents some suggestions for future work.

2

Multicarrier Modulation

Communication systems face many problems when wireless signals are transmitted over the air such as frequency-selective fading, multipath fading, inter carrier interference (ICI), inter-symbol interference (ISI), etc. [10] [11] due to multipath propagation, transmitter or receiver movement, or even changes on channel propagation conditions.

Regarding the transmission over a time-dispersive channel, also known as a frequency-selective channel, the different frequency components of the received signal may experience different levels of fading. To combat this problem, the conventional single-carrier systems require complex equalization schemes [4]. In order to attain an ideal equalization, the frequency response of its equalizer has to be the exact inverse of that of the channel. However, by doing it so, a major problem is raised because, in every transmission over a channel, noise has to be dealt with and such noise can be enhanced through the equalizer whenever a deep fade occurs. As so, even the best equalizer can cause communication failures in single carrier transmission [4].

A solution to deal with frequency-selective fading arises with the proposal to use parallel/multi-carrier (MC) transmission. In a system employing MC transmission, a high-rate serial data stream splits up in several low-rate (thus low-bandwidth) sub-streams, each modulating a different carrier, allowing that only a few sub-channels uses carriers that fall within each deep-faded frequency band. The data corrupted within those corrupted sub-channels can be recovered using error-correcting codes, stressing so its importance in multi-carrier systems [4].

In conventional multi-carrier transmission systems, a few non-overlapping sub-channels share the whole frequency band Fig. 2.1a, allowing possible interference among adjacent sub-channels, known as Adjacent Channel Interference (ACI), to be easily eliminated. However, this guard band between adjacent sub-channels reduces spectral efficiency as it results in a waste of spectrum. Yet, its efficiency can be improved by overlapping the sub-channels by saving a significant amount of spectrum Fig. 2.1b. Towards this end, Orthogonal Frequency Division Multiplexing (OFDM) was developed [4].

(a) Conventional multicarrier technique (b) OFDM technique

Figure 2.1: Resulting bandwidth saving when overlapping sub-carriers.

2.1 OFDM

OFDM can be regarded as either a multiplexing technique or as a special case of multi-carrier modulation which mandates orthogonality in order to avoid ICI [4]. As a multiplexing technique, it allocates sub-channels to an unique frequency range known as the channel bandwidth. The adjacent channels overlap ensuring maximum spectral efficiency. Thus, orthogonality plays an important role since overlapping adjacent channels would interfere with one another. However, sub-carriers in an OFDM system are orthogonal between each other, allowing overlapping without interference.

This parallel transmission scheme provides immunity to selective fading because it divides the overall channel into multiple narrowband signals with the sub-channels bandwidth being adjusted in order to each one of these signals to be affected by flat fading [6]. Since OFDM uses multiple sub-channels, its channel equalization is quite simple, thus reducing the equalizer complexity for each sub-carrier. Although OFDM has such robustness towards a time-dispersive channel it is still affected by its multipath fading. In order to avoid ISI, caused by multipath channel reflections, a cyclic prefix (CP) is added to each individual OFDM symbol as long as its duration is made long compared to that of the delay spread of the time-dispersive channel.

In short, OFDM presents great advantages such immunity to selective fading, resilience to interference, spectrum efficiency, resilience to ISI and simpler channel equalization [12]. Yet, it has some disadvantages. An OFDM signal has a high peak to average power ratio (PAPR), requiring the use of a linear amplifier at the transmitter front-end, that as so cannot operate with high efficiency level [13]. Another constraint is its sensitivity to carrier offset and drifts, while single carrier systems are less sensitive [14]. Finally OFDM suffers from high out-of-band radiation, being in need of a better spectrum confinement, which can be improved using windowing methods [15], however at the cost of an increase of the PAPR. Nonetheless, OFDM is a very popular transmission scheme, adopted in many standards [16] [17] including Digital Audio Broadcasting (DAB), Digital Video Broadcasting (DVB), Asymmetric Digital Subscriber Line (ADSL), Wireless Local Area Network (WLAN), IEEE 802.11 a/g/n, etc. Besides, it is also an important technique for any high data rate transmission over mobile wireless channels. Fig. 2.2 presents a simple OFDM transmission scheme.

2.1.1 OFDM signal

Let $S_l[k]$: $\{k = 0, 1, ..., N-1\}$ be the l^{th} complex symbol to be transmitted by OFDM modulation. Those complex symbols are the result of direct mapping of the original data bits into a selected M-ary signal constellation at rate $1/T_s$. The N serial data stream is

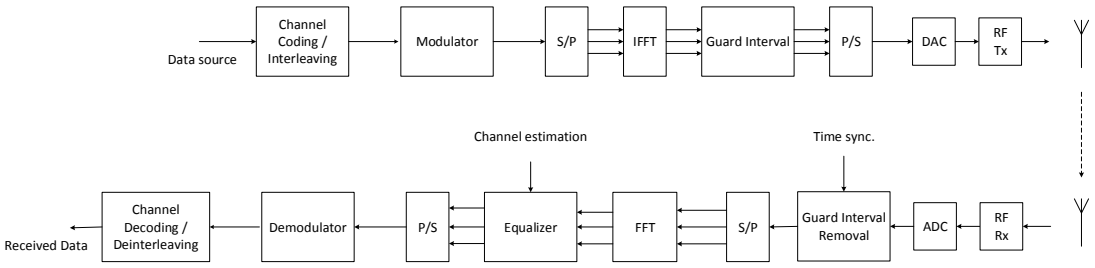

Figure 2.2: Transmission using OFDM.

split up into parallel sub-streams with each one of its N symbols being transmitted by a different sub-carrier. Let's suppose that the k^{th} sub-carrier frequency for $S_l[k]$ is f_k. Then, the modulated OFDM signal can be expressed, in baseband, as [18]

$$s(t) = \sum_{k=0}^{N-1} s_k \varphi_k(t), \tag{2.1}$$

for $0 \leq t \leq T_{sym}$, where

$$\varphi_k = \begin{cases} e^{j2\pi f_k t} & \text{if} \quad 0 \leq t \leq T_{sym} \\ 0 & \text{otherwise} \end{cases} \tag{2.2}$$

and $f_k = f_0 + k\Delta f$ for $k = 0, 1, ..., N-1$. Notice that the transmission time of N symbols is extended, surging a single OFDM symbol. If we consider T_s as the symbol duration at the output of the modulator, $T_{sym} = NT_s$ is called the OFDM symbol duration. As previously stated, OFDM modulation divides the overall frequency-selective fading channel into several narrow band flat fading sub-channels, with $\Delta f = 1/T_{sym}$ being the frequency spacing between OFDM sub-channels.

The overlapping of sub-channels can only be performed as long as its sub-carriers are orthogonal to each other, therefore the receiver can demodulate the OFDM signal. However, the symbol duration must be long enough, such as $T_{sym} = 1/\Delta f$, fulfilling the orthogonality condition.

The complex signals $\{\varphi(k)\}$ represent the different sub-carriers $f_k = f_0 + \Delta f$. Orthogonality condition between sub-carriers can be proved by computing

$$\begin{aligned} &\frac{1}{T_{sym}} \int_0^{T_{sym}} \varphi_k(t) \varphi_l^*(t) dt = \\ &\frac{1}{T_{sym}} \int_0^{T_{sym}} e^{j2\pi(f_k - f_l)t} dt = \\ &\frac{1}{T_{sym}} \int_0^{T_{sym}} e^{j2\pi(k-l)\Delta f t} dt = \delta[k-l], \end{aligned} \tag{2.3}$$

where $\delta[k-l]$ is the delta function *Dirac* sequence defined as

$$\delta[n] = \begin{cases} 1 & \text{if} \quad n = 0 \\ 0 & \text{otherwise} \end{cases} \tag{2.4}$$

We come to conclusion that $\{\varphi(k)\}$ is a set of orthogonal functions.

The received OFDM symbol in baseband can be demodulated, disregarding channel noise, effects by

$$\begin{aligned}
&\frac{1}{T_{sym}}\int_0^{T_{sym}} s(t)e^{-j2\pi f_k t}dt = \\
&\frac{1}{T_{sym}}\int_0^{T_{sym}} \left(\sum_{l=0}^{N-1} s_l\varphi_l(t)\right)\varphi_k^*(t)dt = \\
&\sum_{l=0}^{N-1} s_l\delta[l-k] = s_k,
\end{aligned} \tag{2.5}$$

The previous equation proves that the orthogonality condition allows sub-channels to overlap, wherefore allowing OFDM to achieve high spectral efficiency.

2.1.2 FFT Implementation

Note that we used an integral to demodulate the OFDM signal; however OFDM is well related to the discrete Fourier transform (DFT). As in modern communications, transmitters and receivers are implemented digitally and taking into account that DFT can be implemented by low complexity fast Fourier transform (FFT) with ease, in OFDM transmission schemes, transmitters and receivers can be implemented efficiently by FFT and inverse fast Fourier transform (IFFT), respectively.

As previously discussed, an OFDM signal can be expressed as

$$s(t) = \sum_{k=0}^{N-1} S_k e^{j2\pi f_k t}. \tag{2.6}$$

The output of a digital transmitter is generated by sampling data. By letting $s(t)$ to be sampled at $t = nT_{samp}$, where T_{samp} is the sample interval, then

$$s(nT_{samp}) = \sum_{k=0}^{N-1} S_k e^{j2\pi f_k nT_{samp}}. \tag{2.7}$$

The carrier frequencies should be spaced uniformly in the frequency domain, so let it be $f_s = 1/NT_{samp}$ as the minimum separation in order to keep orthogonality, then $f_k = kf_s$, with $k = 0, 1, ..., N-1$, and, without loss of generality, setting $f_0 = 0$, it results

$$s_n = s(nT_{samp}) = \sum_{k=0}^{N-1} S_k e^{j2\pi nk/N}. \tag{2.8}$$

Observe that the equation 2.8 denotes the inverse discrete Fourier transform. Then, we can write

$$s_n = IDFT\{S_k\}. \tag{2.9}$$

Therefore, it has been proved that the OFDM transmitter can be implemented using IDFT and wherefore it can be efficiently implemented by the FFT algorithm which allows a reduced number of complex multiplications from N^2 to $N/2log_2N$ for an N-point IDFT [19]. Analogously, so does the OFDM receiver can be implemented using the DFT. Such efficient implementations make OFDM a feasible solution to advanced communication systems.

2.1.3 OFDM related issues

2.1.3.A Guard Interval

One of the main issues regarding wireless transmissions over time-dispersive channels is the fading, due to multipath propagation. Although in OFDM multipath fading has been greatly reduced by increasing symbol duration time by N, i.e. $T_{sym} = NT_s$, its effect still threatens the orthogonality condition imposed to the sub-carriers, due to interference between consecutive symbols. This intersymbol interference (ISI) is the result of overlap of the tail part of the actual OFDM symbol with the initial part of the next symbol, due to the time delays on reception resulting from multipath propagation, as shown in Fig. 2.3.

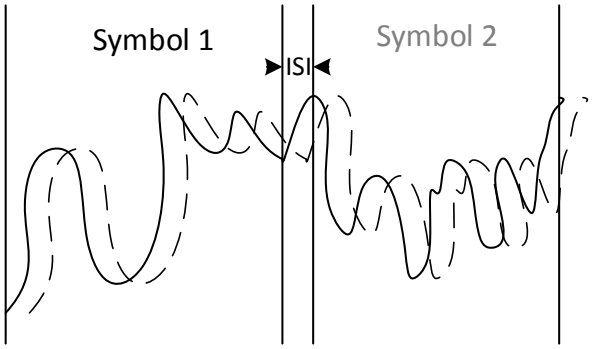

Figure 2.3: Illustration of ISI due to multipath delay.

To deal with delay spreads of wireless channels and thereafter eliminate any possible ISI, usually OFDM systems append a guard band/extension to its OFDM symbols. There are three types of extensions: cyclic prefix (CP), cyclic suffix (CS) and zero-padding (ZP), with this last one depicted in Fig. 2.4.

Cyclic Prefix and Cyclic Suffix

Depending on which cyclic extension is used, the OFDM scheme is designated CP-OFDM or CS-OFDM, either its extension is CP or CS, respectively. The cyclic prefix

is a cyclic extension with length T_g, appended at the beginning of the OFDM symbol, containing a copy of its T_g final samples. Similarly, the cyclic suffix is appended at the end of the OFDM symbol containing a copy of its initial samples. Thus, the OFDM signal $s(t)$, can be extended into $s_g(t)$ by

$$s_g(t) = \begin{cases} s(t) & \text{if} \quad 0 \leq t \leq T_{sym} \\ s(t - T_{sym}) & \text{if} \quad T_{sym} < t \leq T_{sym} + T_g \end{cases} \tag{2.10}$$

This guard interval length T_g is made longer than the delay spread of the wireless channel, therefore the degree of delay spread must be obtained in advance. Note that with the cyclic extension the actual OFDM symbol has its duration increased. The OFDM symbol duration sums up to $T_G = T_{sym} + T_g$. Unfortunately, the guard interval actually wastes transmission resources, by decreasing transmission rate and increasing power consumption, fostering the need to keep a low ratio between the guard interval length, T_g, and the effective OFDM symbol duration, T_{sym}.

Zero-Padding

Another way to add a guard interval between consecutive OFDM symbols is by sending a null waveform by the transmitter during that interval. In another words, it consists in adding a set of zeros at the end part of the OFDM symbol. This scheme is called Zero-Padding (ZP) transmission and it is illustrated in Fig. 2.4.

By adding zeros at the end part of the OFDM symbol we are introducing redundant samples which even having the same duration as a symbol containing CP or CS will require lower transmission power and a simpler transmitter scheme. On the other hand, even though a ZP-OFDM symbol has the same duration as a CP-OFDM or CS-OFDM symbol its effective duration is reduced to the original symbol duration without guard interval. Hence, the signal envelope having lower rectangular shape duration means a wider *sinc* shaped spectrum, thereby its power spectral density exhibits smaller ripple.

However, the ZP-OFDM scheme introduces ICI, caused by the multiple copies of the time-shifted ZP-OFDM symbol received due to multipath propagation, which breaks the orthogonality condition among sub-carriers and complicates receiver design. This cause CP-OFDM and CS-OFDM schemes to be preferable due to its capability of removing ICI.

Signal Detection

Anyhow, the interval guard provides OFDM systems to achieve quite simple signal detection, being one of the reasons on why OFDM is so popular. As explained above, an

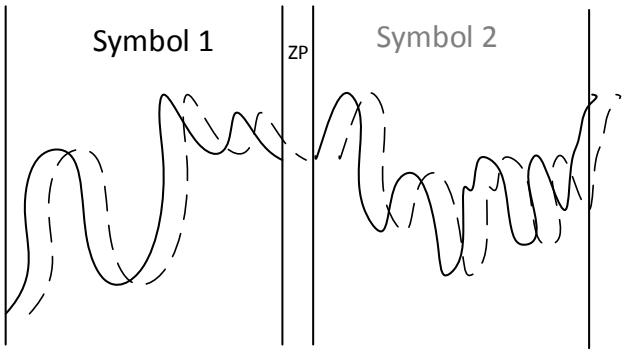

Figure 2.4: Zero-padding guard interval to avoid ISI.

cyclic extended OFDM symbol can be expressed as

$$s_g(t) = \sum_{k=0}^{N-1} s_k e^{j2\pi f_k t} \tag{2.11}$$

where $-T_g \leq t \leq T_{sym}$. To study the impact of the channel at the CP-OFDM system, let's commence by expressing its impulse response,

$$h(t) = \sum_i \gamma_i \delta(t - \tau_i), \tag{2.12}$$

where γ_i and τ_i are the delay and complex amplitude of the i^{th} path, respectively. The received signal is the result of the convolution of the CP-OFDM signal, $s(t)$, and the channel impulse response, $h(t)$, i.e. $(s(t) * h(t))$ plus noise,

$$y(t) = \sum_i \gamma_i s_g(t - \tau_i) + n(t) \tag{2.13}$$

where $n(t)$ is the additive white Gaussian noise (AWGN) at the receiver. The interval guard allows the received signal to avoid having signals from different OFDM blocks. If the duration of the CP extension is greater than the delay spread, no ISI occurs in the interval $0 \leq y \leq T_{sym}$ and the received signal is

$$Y_k = \frac{1}{T_{sym}} \int_0^{T_{sym}} y(t) e^{-j2\pi f_k t} dt, \tag{2.14}$$

by replacing $y(t)$ in the previous equation for equation, it results

$$Y_k = H_k S_k + N_k, \tag{2.15}$$

for $k = 0, 1, ..., N-1$, where H_k is defined as

$$H_k = \sum_i \gamma_i e^{-2\pi k \Delta f \tau_i}, \tag{2.16}$$

denoting the frequency response at the k^{th} sub-channel and N_k is defined as

$$N_k = \frac{1}{T_{sym}} \int_0^{T_{sym}} n(t) e^{-j2\pi f_k t} dt, \tag{2.17}$$

denoting the impact of AWGN at the same sub-channel.

Equation clearly show that the channel's impact is only a multiplicative distortion at each sub-channel of the OFDM system [20] allowing simple signal detection as previously stated.

2.1.3.B Null Sub-carriers

In OFDM transmission schemes over wireless channels, it often occurs ICI and leakage to adjacent bands. To prevent it, OFDM systems usually have the sub-carriers near the two edges of the assigned band unused. Those are known as guard sub-carriers or virtual sub-carriers. All these unused sub-carriers constitute a frequency domain guard band [4].

The OFDM signal power spectrum has quite high sidelobes, meaning it has significant out-of-band power emission, which is undesirable because it increases the requirements on transmitter front-end filters. The additional frequency domain guard interval helps to reduce the out-of-band emission. However, this guard band wastes valuable bandwidth, hence decreasing spectral efficiency.

Another addition to this guard band supplied by virtual sub-carriers are some unused sub-carriers around DC frequency. The point of keeping those null is to evade unwanted DC and low frequency components generated by the receiver front-end.

2.1.3.C Spectrum

The modulated OFDM symbol can be expressed by equation, however, as it has been mentioned previously, its signal envelope has rectangular shape due to the applied rectangular pulse and so we can write

$$s(t) = \sum_{k=0}^{N-1} S_k w(t) e^{j2\pi f_k t}, \tag{2.18}$$

where $w(t)$ is a unit rectangular pulse having the same duration time, T_{sym}, as the original modulated OFDM symbol. The above equation can be seen as a summation of truncated complex exponential functions with different frequencies, thereby its power density spectrum consists of a superposition sum of shifted *sinc* shaped spectra ($|\sin f/f|$), each centered at a different sub-carrier frequency f_k.

Fig. 2.5 presents a sketch of the normalized power density spectrum of an OFDM symbol with N sub-carriers versus the normalized frequency fT_s. The first sub-carrier is

illustrated by the dotted curve. Its shape gives an idea of the overall power density spectra, constructed summing all N individual power density spectra.

Note that only sub-channels near the edges contribute to out-of-band power emission. Therefore, as long as N is made large, the power density spectrum approaches that of single-carrier modulation.

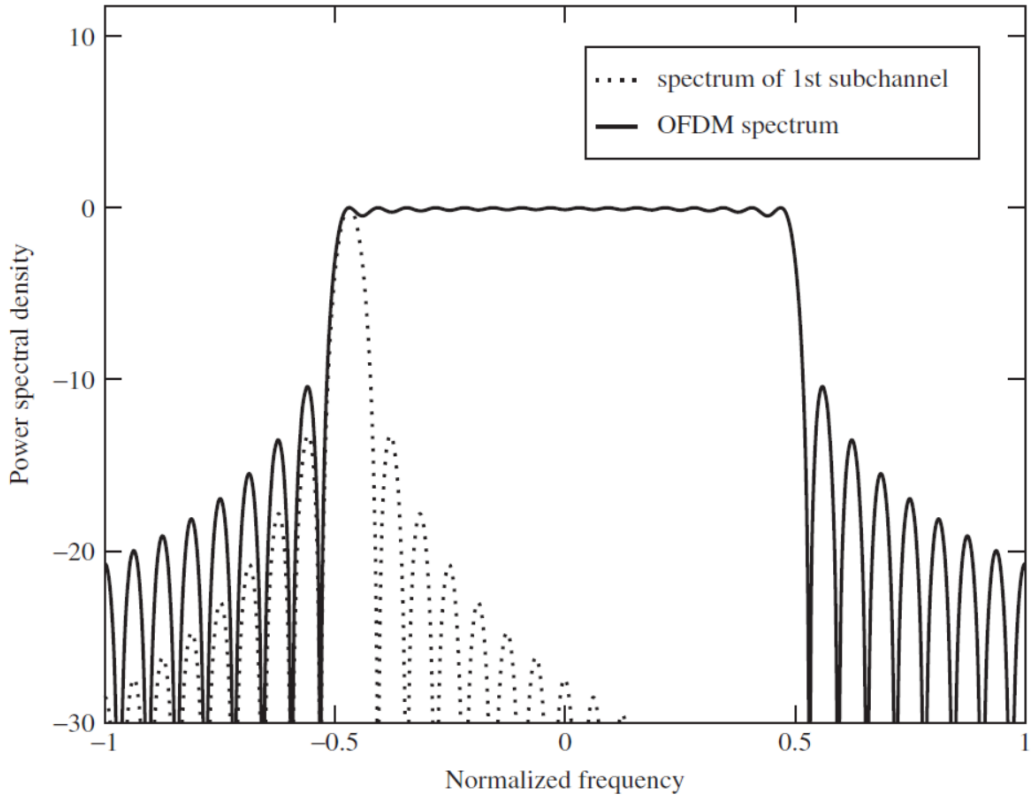

Figure 2.5: OFDM spectrum [1].

For an OFDM signal consisting of N sub-channels, the signal bandwidth can be approximated by $(N+1)\Delta f$. Each sub-channel has a transmission rate of $1/T_{sym}$ symbols/sec leading to a total transmission rate of N/T_{sym} symbols/sec. Thus, the bandwidth efficiency of the OFDM system is [18].

$$\eta = \frac{N/T_G}{(N+1)\Delta f} = \frac{N/(T_{sym}+T_g)}{(N+1)/T_{sym}} = \frac{1}{1+\frac{1}{N}} \frac{1}{1+\frac{T_g}{T_{sym}}} \tag{2.19}$$

with η in symbols/sec/Hz.

2.1.3.D PAPR

A major weakness for OFDM communication systems is its common large fluctuations in signal envelope. This unfortunate outcome is valued by the peak-to-average

power ratio (PAPR). This parameter is defined as the ratio between the signal peak and average power, or by its formula [13]

$$PAPR = \frac{max|s(t)|^2}{E\{|s(t)|^2\}}. \tag{2.20}$$

As previously mentioned, the OFDM system improves as the number of sub-carriers is made as big as possible. However, if we consider the extreme case in which all those sub-carriers are coherently and equally summed up, the PAPR can be as high as N.

A high PAPR as a critical impact on power amplifiers (PA), especially those located at the transmitter. Such PAPR demands high dynamic range in PAs, causing them to easily enter in saturation, if not biased properly. A power amplifier in saturation frequently acts as a nonlinear amplifier when dealing with large magnitude signals. To accommodate such signals linearly, the PA must work at an operating point, $P_{o,avg}$, which is inefficient in terms of power consumption. This implies the implementation of a large output back-off (OBO), which is defined as the output saturation power to the average output power of a power amplifier, expressed as

$$OBO = 10log_{10}\frac{P_{o,max}}{P_{o,avg}}(dB). \tag{2.21}$$

Many approaches tempting to reduce PAPR have been proposed. One of the solutions is to use linearisation techniques to increase the dynamic range of the amplifier. Other approaches consist in clipping and windowing the peak signals [21], partial transmit sequence [22] and selective mapping techniques [23]. However, those techniques may introduce in-band distortion and out-of-band radiation as well as raising the complexity of the system.

2.1.4 Equalization

The most popular linear equalization criteria are Zero-Forcing (ZF) and Minimum Mean Square Error (MMSE).

Zero-Forcing

The ZF criteria is simpler than the MMSE criteria. Its purpose is to invert the channel frequency response, being its coefficients expressed as

$$G[k] = \frac{H^*[k]}{|H[k]|^2}, \tag{2.22}$$

where H_k denotes the channel frequency response.

Although ZF is quite simple to implement, it isn't the most appropriate to deal with deep fading. In transmission over dispersive channels deep fade often occurs, imposing $H[k] \approx 0$ which leads to an overlap of the noise above the transmitted symbol as it can be described in the following equation

$$\begin{aligned}\tilde{X}[k] &= Y[k]G[k] \\ &= X[k]H[k]G[k] + Z[k]G[k] \\ &= X[k]H[k]\frac{H^*[k]}{|H[k]|^2} + Z[k]\frac{H^*[k]}{|H[k]|^2} \\ &= X[k] + Z[k]\frac{H^*[k]}{|H[k]|^2}.\end{aligned} \tag{2.23}$$

where $\tilde{X}[k]$ is the estimate of the transmitted symbol $X[k]$.

MMSE

The MMSE criteria consists in minimizing the quadratic error $E\left\{|\tilde{X}[k] - X[k]|^2\right\}$, having its coefficient given by

$$G[k] = \frac{H^*[k]}{\frac{1}{\gamma} + |H[k]|^2}, \tag{2.24}$$

where γ represents the signal-to-noise ratio (SNR).

This criteria efficiently faces the channel deep fading problem, as one can see from eq. 2.33, where noise disappears for low SNR values.

2.2 Block-Windowed Burst OFDM: A High Efficiency Multicarrier Technique

In this section, the new transceiver scheme proposed in [3] [2], designated *Block Windowed Burst OFDM* (BWB-OFDM), is presented.

This multicarrier technique has a power spectral density (PSD) similar to the filtered OFDM approach, employing smoother, non-rectangular windows. The system description is divided in three main subjects: the architecture of transmitter and the receiver and the comparison of the performance of the BWB-OFDM transceiver to typical CP-OFDM schemes.

2.2.1 Introduction

The previous section clearly stressed why OFDM schemes are very popular now-a-days, mainly due to its effectiveness in combating the frequency selective fading that normally occurs in wireless transmissions, while allowingfor high speed data transmissions. Although such popular technique shows quite good bit-error rate (BER) performance, low complexity and robustness over multipath propagation, the OFDM trasmission scheme faces a main constrain, the high level of the side lobes of its signal spectrum, i.e. spectrum leakage.

The principal motivation for the new transceiver scheme BWB-OFDM is to achieve greater signal spectrum confinement keeping the low complexity that typical OFDM systems guarantee. This is achieved by either improving spectral confinement compared to an CP-OFDM system operating at the same transmission rate and for the same number of carriers, or by achieving higher transmission rates for the same spectrum characteristics of conventional OFDM.

The superior spectrum confinement is assured by using windowing techniques in which each OFDM symbol is cyclic extended and windowed at the time-domain by a square-root raised cosine (SRRC), at the transmitter, and, at the receiver, after equalization, each one of those windowed symbols get applied the same window (matched filtering) in order to reject any ICI. In addition, instead of using, systematically, a CP between symbols (as in CP-OFDM), the BWB-OFDM system applies a sole guard interval (ZP) to a set of consecutive N_s windowed-OFDM symbols, with emphasis being put at the frequency domain equalization (FDE) performed at the receiver that treats the burst received signal (i.e. set of N_s consecutive symbols) as of a block-based SC transmission type.

The new transceiver scheme allows as so a commitment between better signal spectrum confinement and a higher transmission rate. The commitment allows BWB-OFDM to achieve transmission rates up to 11% higher than typical OFDM schemes by keeping its rectangular symbol configuration or to keep the same transmission rate as OFDM but attain 35-45 dB of gain in spectral confinement depending on the window's *roll-off* [2]. Another important aspect of this transceiver technique is its increase in energy efficiency towards typical CP-OFDM systems, given that a sole ZP guard interval is used per N_s symbols.

BWB-OFDM can thus be categorized as a hybrid block transmission scheme, since this new scheme is similar to a typical OFDM scheme from the transmitter side and to a SC-FDE scheme from the receiver.

2.2.2 Transmitter

The new transceiver scheme BWB-OFDM proposes a transmitter built on the filtered OFDM scheme [3]. The main idea as in the filtered-OFDM technique [24] is to control the power spectral density (PSD) of the signal to transmit, i.e., it pretends to achieve a PSD with lower out-of-band radiation.

For the purpose of describing the BWB-OFDM transmitter, consider a sequence of N modulated symbols, resulting from direct mapping of a binary sequence into a selected constellation (e.g. Quadrature Phase Shift Keying (QPSK)). As we pretend to ensure a robust transmission over a wireless time-dispersive channel, channel coding and interleaving are applied to the considered binary sequence, prior to modulation.

As in a conventional OFDM, those modulated symbols are subsequently converted into N parallel streams of lower rate each modulating a different sub-carrier. The complex envelope of a baseband conventional OFDM symbol can be expressed in discrete time domain as

$$s_n = \sum_{k=0}^{N-1} S_k w[n] e^{j2\pi kn/N}, \tag{2.25}$$

where $n = 0,1,...,N-1$, $S_k : \{k = 0,1,...,N-1\}$ denotes the modulated symbols at the k^{th} sub-carrier and $w[n]$ is a unit rectangular pulse with length N. Note that the orthogonality condition is assured by keeping the frequency spacing between adjacent sub-carriers equal to $1/N$. Also the equation turns out to be the N-point IDFT of the modulated symbols S_k and can be computed efficiently by using the IFFT algorithm.

So far, the description of the transmitter resembles a typical OFDM transmitter since the BWB-OFDM is built on the filtered-OFDM scheme. However, as stated previously, OFDM systems present high levels of out-of-band radiation, causing ICI, due to the rectangular window that has a *sinc* shaped spectrum with high side lobes. In filtered-OFDM signals, in order to get a better spectrum confinement, conventional filtering techniques can be used. However, although having less control over spectral confinement than filtering, windowing results to be more convenient and appropriated because it requires just a few multiplications over the samples that fall-off into the *roll-off* region. This reduction of complexity can go as far as one order of magnitude [19].

The desired spectrum can be achieved applying a window with reduced frequency side lobes such as a square-root raised cosine (SRRC) window. In order to do so, first cyclic extension is applied to the OFDM symbol and only then the rectangular window $w[n]$ is applied. Fig. 2.6 shows the considerable gains obtained in spectrum confinement by the

use of SRRC windows with different *roll-offs*, whose expression for a given *roll-off*, β, is

$$h_{SRRC}[n] = \begin{cases} 1 & , \quad |n| \leq \frac{N}{2}(1-\beta) \\ \cos\left(\frac{\pi}{4\beta}\left[\frac{2n}{N} - (1-\beta)\right]\right) & , \quad \frac{N}{2}(1-\beta) \leq |n| \leq \frac{N}{2}(1+\beta) \\ 0 & , \quad |n| \geq \frac{N}{1}(1+\beta) \end{cases} \tag{2.26}$$

where $n = -N, ..., N$.

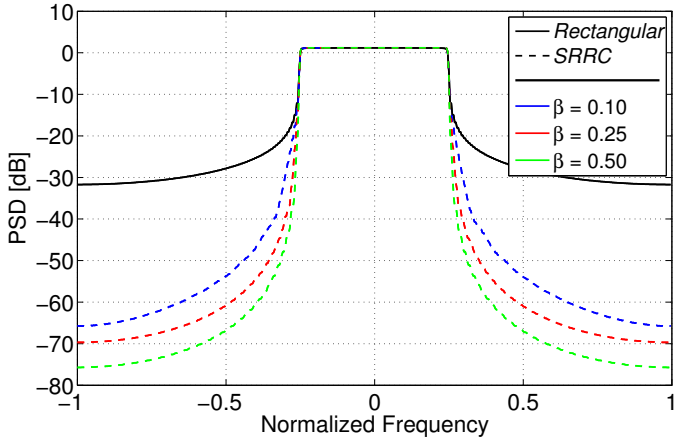

Figure 2.6: PSD of the transmitted signal apllying a SRRC window [2].

Mathematically, the windowing of the symbol s_n results in a new symbol that may be written in matrix form as

$$\mathbf{s}_w = [\quad \mathbf{s}_n \quad | \quad \mathbf{s}_n \quad]_{(1\times 2N)} \odot \mathbf{h}_{SRRC_{(1\times 2N)}}, \tag{2.27}$$

where the operator $\odot$ represents a point-wise product and bold lettering is used to denote a vector, i.e. $\mathbf{x}_{(1\times N)} = [x_0 ... x_{N-1}]$.

The window adoption allows a better spectrum confinement at the cost of an increase of the samples per transmitted symbol to $N(1+\beta)$ (bordering zeros resulting from the $\odot$ product are discarded). Although the increase in transmitted samples per symbol, the symbol energy remains the same due to $h_{SRRC}[n]$ shape. This results in a considerable power efficiency gain compared to CP-OFDM, because as stated before in BWB-OFDM, N_s symbols are packed together with no guard-band between each other. Note that in a CP-OFDM system there is a waste of power, with an efficiency loss of

$$\varepsilon = N/(N+N_{cp}), \tag{2.28}$$

However, when transmitting over a wireless time-dispersive channel, there is the need to deal with its delay spread so there is also the need to add a guard interval. In BWB-OFDM, a ZP qith length N_{zp} is added only at the end of a block of N_s symbols s_w. N_{zp} is chosen as to be longer than the delay spread of the multipath channel, while proper value of N_s stresses from the complexity put on the receiver's equalizer.

The resulting BWB-OFDM symbol can be written as

$$\mathbf{x}_n = [\quad \mathbf{s}_B \quad | \quad \mathbf{0}_{(1\times N_{zp})} \quad]_{(1\times N_x)}, \tag{2.29}$$

where $\mathbf{0}_{(1\times N_{zp})}$ represents a null vector of length N_{zp}, $N_x = N_s \times N(1+\beta)+N_{zp}$, and

$$\mathbf{s}_B = [\quad \mathbf{s}_{w,1} \quad | \quad \mathbf{s}_{w,2} \quad | \quad \ldots \quad | \quad \mathbf{s}_{w,N_s} \quad]_{(1\times N_B)}, \tag{2.30}$$

is a set of symbols $\mathbf{s}_{w,j}$ packed together as a mega block with j denoting the symbol index and $N_b = N_s \times N(1+\beta)$.

The resulting mega block $\mathbf{s}_B$ can be efficiently generated by N_s parallel streams, as depicted in Fig. 2.7.

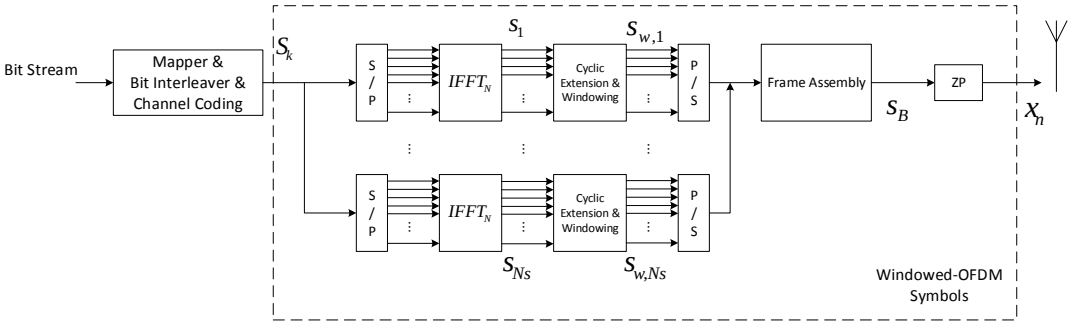

Figure 2.7: Diagram of BWB-OFDM transmitter.

2.2.3 Receiver

Fig. 2.8 presents the block diagram of the BWB-OFDM receiver. The received time-domain block y_n, with length N_x is first converted to the frequency domain. The received block in the frequency domain, Y_k, is obtained by a N_x-sized DFT, implemented through the efficient FFT algorithm. When considering that the length of the guard interval ZP, N_{zp} is made longer than the delay spread of the channel, Y_k can be written as

$$Y_k = H_k X_k + N_k, \tag{2.31}$$

with $X_k = DFT\{x_n\}$, where DFT denotes the discrete Fourier transform, and H_k and N_k denote, at the k^{th} sub-carrier, the channel frequency response and the complex additive white Gaussian noise (AWGN), respectively.

As previously stated, OFDM schemes offer quite simple equalization processes because it allows the division of the dispersive channel in many parallel, low-rate, flat fading channels, enabling low complexity and fast forward implementation of a linear frequency

domain equalization (FDE).

Equalization

ZF or MMSE techniques used in OFDM can also be employed with the equalized signal being given by

$$\hat{\mathbf{X}}_k = \frac{\mathbf{Y}_k \mathbf{H}_k^*}{|\mathbf{H}_k|^2} \tag{2.32}$$

and

$$\hat{\mathbf{X}}_k = \frac{\mathbf{Y}_k \mathbf{H}_k^*}{\frac{1}{\gamma}|\mathbf{H}_k|^2} \tag{2.33}$$

, respectively.

After equalization, it follows the conversion of $\hat{X}_k$ back to time-domain by the means of a N_x-sized IFFT, i.e. $\hat{x}_n = IFFT\left\{\hat{X}_k\right\}$. The cyclic extension ZP is removed and it is followed by a serial-to-parallel conversion, which separates the megablock $\hat{x}_n$ without the ZP into N_s symbols with length $N(1+\beta)$.

In order to apply the same windowing process (matched filtering), avoiding possible ACI, a equal number of zeros is added at both ends of each symbol $\hat{x}_{n,j}, j = 1,...,N_s$, enough to increase its length up to $2N$.

The result of matched filtering can be expressed as

$$\hat{s}_{w,j} = \hat{x}_{n,j(1\times 2N)} \odot \mathbf{h}_{SRRC(1\times 2N)}. \tag{2.34}$$

The resulting estimated BWB-OFDM symbols, $\hat{s}_{w,j}$, are then converted back to frequency-domain by the means of a $2N$-sized FFT, i.e. $\hat{S}_{w,j} = FFT\left\{\hat{s}_{w,j}\right\}$ and downsampled by 2.

The final result yields the estimates of the original S_k data of the j^{th} OFDM symbol, given by

$$\hat{S}_{k,j}[i] = \hat{S}_{k,j}[2i]_{(1\times 2N)}, \tag{2.35}$$

with $i = 0,1,...,N-1$.

At last, to get the original bit stream data, on each $\hat{S}_{k,j}$ it is applied the original bit deinterleaving and channel decoding.

2.2.4 BWB-OFDM versus CP-OFDM

The proposed scheme, BWB-OFDM, presents a gain of about 2dB over a typical CP-OFDM setting. This BER performance, achieved for time-dispersive channels, is inherent to the transmitter structure, where no CP is used.

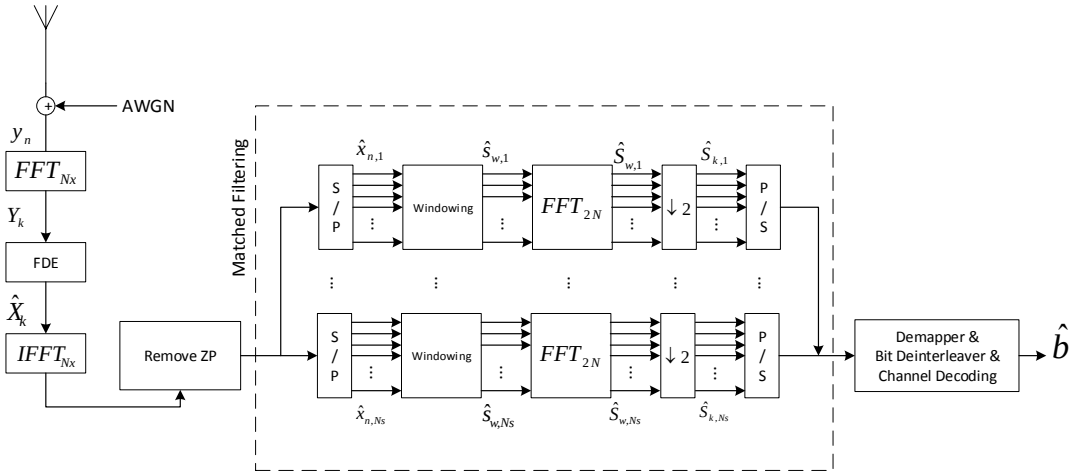

Figure 2.8: Diagram of BWB-OFDM receiver.

Further, the windowing technique applied, allows an increase to the transmission rate, depending on the window's *roll-off* (β). This transmission rate is given by

$$\kappa = \frac{N_s \times N \times \beta}{Nx} \times 100\%, \tag{2.36}$$

where N_x is the total length of the BWB-OFDM block, N is the number of sub-carriers and N_s is the number of symbols per block. Thus, the BWB-OFDM scheme allows a commitment between spectral confinement and transmission rate, keeping an almost identical BER performance, Fig. 2.9.

In addition, experimental results have shown that the BWB-OFDM scheme allows a gain up to 0.5dB PAPR related [2].

Concluding, the BWB-OFDM looks promising and it is the subject of this thesis, having as its main goal to achieve performances near the theoretical limit (*Matched Filter Bound*) by developing more sophisticated receivers. The research was focused on the recent popular IB-DFE receiver which will be briefly explained in the subsequent chapter.

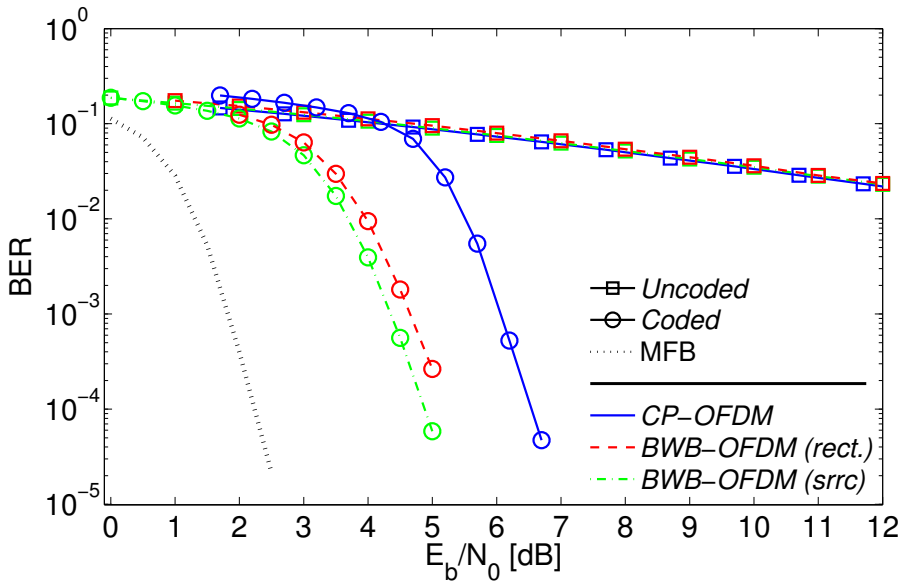

Figure 2.9: BER results for OFDM and BWB-OFDM with rectangular and SRRC windowing, both coded and uncoded transmissions, over dispersive channel [3].

3

Iterative Block Decision Feedback Equalization

A high data rate transmission over severely time-dispersive channels requires a system capable of dealing with those time-dispersion effects associated to the multipath propagation. In order to suit that requirement, it has been shown that block transmission techniques with appropriated cyclic prefix (CP) and employment of frequency-domain equalization techniques are the best option [25] [26]. The most popular techniques are OFDM (Orthogonal Frequency Division Multiplexing) and SC-FDE (Single-Carrier Frequency Domain Equalization) but the presented scheme BWB-OFDM proved to be a flexible alternative with great performance. Typically, the receiver for those schemes is a linear FDE. However, for SC-FDE schemes, a nonlinear equalizer offers much better performance [27]. Its performance can be very close to Matched Filter Bound (MFB) [28], so nonlinear equalizers are much more interesting. A promising nonlinear equalizer is the Iterative Block Decision Feedback Equalizer (IB-DFE) [29]. Although this iterative FDE technique only applies to SC schemes, thus excluding OFDM techniques, in the new BWB-OFDM transceiver scheme the received signal can be regarded as of an SC-FDE type. Thus, intending to achieve performances close to MFB, this chapter outlines the scheme of an IB-DFE receiver.

3.1 Basic IB-DFE Receiver

The IB-DFE receiver is an iterative FDE with feedforward and feedback filters. These are implemented in the frequency domain and each one aim for different purposes. The feedforward filter partially equalizes the channel, assuming perfect channel knowledge. On the other hand, the feedback filter minimizes the intersymbolic interference (ISI) and removes part of the residual interference due to previous estimations. The basic IB-DFE structure is presented below, Fig. 3.1.

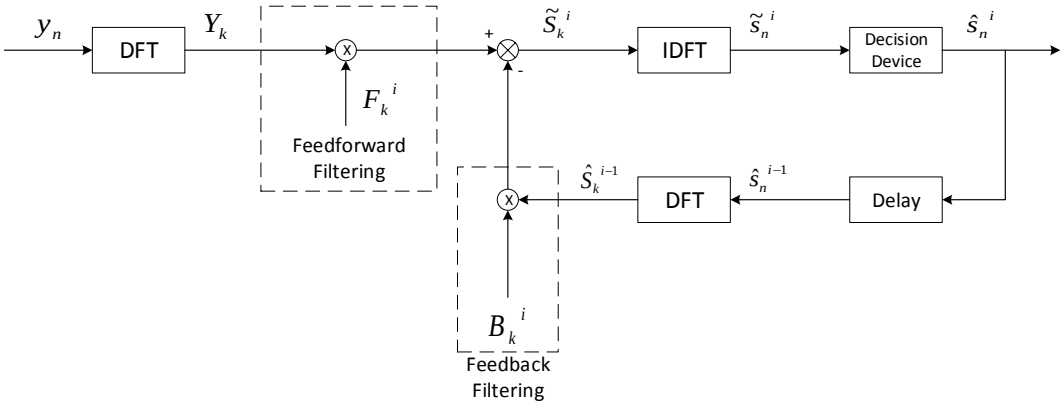

Figure 3.1: Block diagram representation of a basic IB-DFE receiver.

With the basic knowledge on how IB-DFE works we proceed to describe how to compute the feedforward and feedback filter coefficients as well as to describe the whole system.

3.1.1 Basic Receiver Structure

In order to deliver a full description of the IB-DFE receiver we consider a SC-FDE modulation scheme which allows a simple description of the whole system making it easier to understand its appliance to the BWB-OFDM scheme presented in the subsequent chapter. Thus, the data is transmitted in blocks of N modulated symbols, of an M-ary constellation (e.g. QPSK, 16-QAM, etc.) , with a suitable cyclic prefix (CP), that accommodates channel time-dispersion, resulting in $x_n : \{n = 0, 1, ..., N-1\}$. For sake of simplicity consider, at reception, perfect channel estimation and assume that the received signal has been previously matched filtered, sampled and had its CP removed. The received block y_n with N time domain samples is converted to the corresponding frequency-domain block by an appropriate size-N discrete Fourier transform (DFT) resulting in Y_k with N frequency domain samples, where $Y_k : \{k = 0, 1, ..., N-1\}$ can be written as

$$Y_k = H_k X_k + N_k, \tag{3.1}$$

where X_k is the N-sized FFT of the transmitted block x_n, H_k denotes the overall channel frequency response for the k^{th} frequency and N_k represents the corresponding channel AWGN noise in frequency domain.

Next, we proceed to deal with the channel effects by replacing the linear FDE, employed in most SC-FDE schemes, by an IB-DFE. For ease of reference, keep in mind its basic structure depicted in Fig. 3.1. At the output of the equalizer, for the i^{th} iteration, the frequency-domain block $\tilde{S}_k^{(i)}$ with $k = 0, 1, ..., N-1$ can be written as

$$\tilde{S}_k^{(i)} = F_k^{(i)} Y_k - B_k^{(i)} \hat{S}_k^{(i-1)}. \tag{3.2}$$

where $F_k^{(i)} : \{k = 0, 1, ..., N-1\}$ and $B_k^{(i)} : \{k = 0, 1, ..., N-1\}$ are the coefficients of the feedforward and feedback filters, respectively. $\hat{S}_k^{(i-1)} : \{k = 0, 1, ..., N-1\}$ are the DFT samples of the estimated block $\hat{s}_n^{(i-1)} : \{n = 0, 1, ..., N-1\}$ after the decision device, denoting the estimation of s_n from the previous iteration $(i-1)$.

The feedforward an feedback filter coefficients are computed in order to maximize the overall signal to interference plus noise ratio (SINR) by minimizing the mean squared error (MSE) of the received signal [30]. It can be shown that the optimal feedforward and feedback filter coefficients are, respectively,

$$F_k^{(i)} = \frac{\kappa H_k^*}{\frac{1}{\gamma} + \left(1 - (\rho_m^{(i-1)})^2\right) |H_k|^2}, \tag{3.3}$$

and

$$B_k^{(i)} = \rho \left(F_k^{(i)} H_k - 1 \right), \tag{3.4}$$

where γ represents the signal-to-noise ratio (SNR) and κ is a normalized constant selected to guarantee that $\frac{1}{N}\sum_{k=0}^{N-1} F_k^{(i)} H_k = 1$.

The key parameter for good performance of the IB-DFE receiver is the correlation factor, ρ. This parameter is a measure of the blockwise realiability of the estimates from the previous iteration, i.e. $\hat{s}_n^{(i-1)}$, employed in the feedback loop. The correlation factor ρ is defined as

$$\rho_m^{(i-1)} = \frac{E\left[\hat{s}_n^{i-1} s_n\right]}{E\left[|s_n|^2\right]} = \frac{E\left[\hat{S}_k^{i-1} S_k\right]}{E\left[|S_k|^2\right]}, \tag{3.5}$$

and can be computed on the time or frequency domain.

Although the exact computation of ρ depends on the knowledge of the transmitted signal x_n (which in fact is the aim of the equalization procedure), a good aproximation can be computed as [31]

$$\rho_m^{(i-1)} = \frac{E\left[\hat{s}_n^{i-1} \tilde{s}_n\right]}{E\left[|\tilde{s}_n|^2\right]}, \tag{3.6}$$

with $\tilde{s}_n$ the obtained signal at the output of the feedforward filter.

As previously stated, ρ provides a measure of the blockwise reliability between the output of the equalizer, $\tilde{S}_k$ and the estimate given by the decision device $\hat{S}_k$.

3.1.2 Decision Device

The decision device is an important part of the IB-DFE system used in the feedback loop. Its purpose is to provide block estimates with the best effort in order to offer a good measure of the blockwise reliability provided by ρ. Since inaccuracy of the data estimation affects the overall performance of the system, the decision device plays an important role.

Two type of decisions can be taken: ”hard” or ”soft”. For an M-ary constellation, and given a estimated symbol $\tilde{s}_s$, a hard decider based on a minimum distance criteria, chooses the constellation symbol (among the M possible candidates) that is closer to $\tilde{s}_s$.

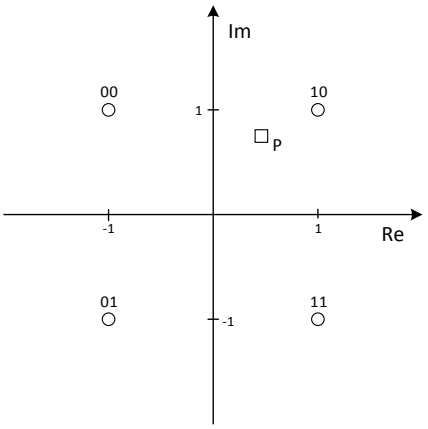

Figure 3.2: QPSK constellation with Gray coding associated.

Following the example of a QPSk constellation in the above figure, when using "hard decisions", the decision device estimates the received symbol p by the sign of its real and imaginary parts. As both are positive, the estimated symbol, $\hat{p}$ yields (1+1j).

However, "soft decision" can improve accuracy of IB-DFE ρ computation. In this case, instead of taken a "fixed" decision on each bit that composes a symbol, it is computed a log-likelihood probability for each bit.

3.1.3 IB-DFE with Soft Decisions

Under the "soft decision" condition the "blockwise average" is substituted by "symbol averages", i.e., the estimates reliability are evaluated symbol by symbol instead of a blockwise measure. Then, the hard decisions $\hat{s}_n$ are replaced for $\bar{s}_n$, denoting the data estimations for IB-DFE with "soft decisions".

Considering as an example a normalized constellation QPSk with Gray mapping $(\pm 1 \pm 1\,j)$ yielding $s_n^I = Re\{\pm 1\}$ and $s_n^Q = Im\{\pm 1\}$ for the "in-phase bit" and "quadrature bit", respectively, the, *soft decisions* can be computed separately and we may write [32]

$$\bar{s}_n^{I(i)} = \tanh\left(\frac{\Lambda_n^{I(i)}}{2}\right) \tag{3.7}$$

and

$$\bar{s}_n^{Q(i)} = \tanh\left(\frac{\Lambda_n^{Q(i)}}{2}\right) \tag{3.8}$$

where $\Lambda_n^{I(i)}$ and $\Lambda_n^{Q(i)}$ are the Log-likelihood Ratios of the "in-phase bit" and the "quadrature bit".[1]

[1]For the sake of understanding, explanation of IB-DFE with *soft decisions* is restricted to the analysis

The LLRs are decribed as

$$\Lambda_n^{I(i)} = \frac{2Re\left\{\tilde{s}_n^{(i)}\right\}}{\sigma_N^2} \tag{3.9}$$

and

$$\Lambda_n^{Q(i)} = \frac{2Im\left\{\tilde{s}_n^{(i)}\right\}}{\sigma_N^2} \tag{3.10}$$

where $\tilde{s}_n^{(i)}$ is the output of the equalizer and σ_N^2 is the total variance of interference and channel noise, given by

$$\sigma_N^2 = \frac{1}{2}E\left[\left|s_n - \tilde{s}_n^{(i)}\right|^2\right] \approx \frac{1}{2N}\sum_{n=0}^{N-1}\left|\hat{s}_n^{(i)} - \tilde{s}_n^{(i)}\right|^2. \tag{3.11}$$

Note that the *hard decisions*, $\hat{s}_n^I = \pm 1$ and $\hat{s}_n^Q = \pm 1$, are defined by the signs of Λ_n^I and Λ_n^Q, respectively.

At this point we can write *soft decisions* as

$$\bar{s}_n^{(i)} = \tanh\left(\frac{\Lambda_n^{I(i)}}{2}\right) + j\tanh\left(\frac{\Lambda_n^{Q(i)}}{2}\right) = \rho_n^I \hat{s}_n^I + j\rho_n^Q \hat{s}_n^Q, \tag{3.12}$$

As previously stated, the correlation coefficient is a major key for good performance and it offers reliabilities denoted by ρ_n^I, for "in-phase bit", and ρ_n^Q, for "quadrature bit", for the n^{th} symbol. These reliabilities are given by

$$\rho_n^{I(i)} = \left|\tanh\left(\frac{\Lambda_n^{I(i)}}{2}\right)\right|, \tag{3.13}$$

and

$$\rho_n^{Q(i)} = \left|\tanh\left(\frac{\Lambda_n^{Q(i)}}{2}\right)\right|. \tag{3.14}$$

The blockwise correlation factor, employing *soft decisions*, that is used in 3.3 for computing feedforward filter coefficient F_k, is then given by

$$\rho_m^{(i)} = \frac{1}{2N}\sum_{n=0}^{N-1}\left(\rho_n^{I(i)} + \rho_n^{Q(i)}\right), \tag{3.15}$$

for the m^{th} time block at the i^{th} iteration.

Although the feedforward filter coefficients, $F_k^{(i)}$, are still given by the same equation 3.3, computation of $B_k^{(i)}$ can be simplified. In fact we can write

$$B_k^{'(i)} = B_k^{(i)} / \rho_m^{(i-1)}, \tag{3.16}$$

of the QPSK case (as usually done in literature). However similar analysis can be conducted for general constellations [33].

and

$$\bar{S}_k^{(i)} = \rho_m^{(i-1)} \hat{S}_k^{(i-1)}, \tag{3.17}$$

(as the "blockwise average" was substituted by "symbol averages"), the feedback filter coefficients $B_k^{(i)}$, are given by

$$B_k^{(i)} = F_k^{(i)} H_k - 1. \tag{3.18}$$

At last, we can obtain the estimated data symbols, computed as

$$\tilde{S}_k^{(i)} = F_k^{(i)} Y_k - B_k^{(i)} \bar{S}_k^{(i-1)}. \tag{3.19}$$

Obviously, for the first iteration, $\hat{s}_m^{(i)} = 0$, due to $\rho_m^{(0)} = 0$. It is easy to notice that, at the first iteration, the equalizer can be considered a linear FDE since there is no feedback loop estimation to account for.

3.2 Turbo IB-DFE

When channel coding is used, transmission systems get a substantial improvement in its overall performance, namely in its BER performance. Furthermore, when dealing with time-dispersive channels, coding is indispensable to recover data corrupted by deep-faded frequency bands. Usually, decoding is done after the equalization, either linear or nonlinear. However, when IB-DFE is integrated with coding/decoding, a much better performance is expected. Decoding can be carried in the IB-DFE loop, being denoted by turbo equalization in the frequency domain (FD), see Fig. 3.3.

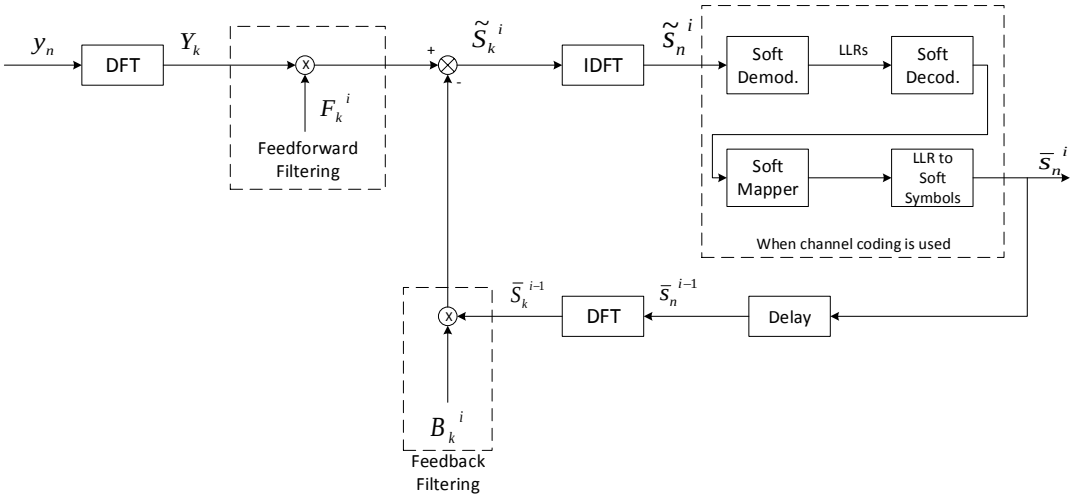

Figure 3.3: Block diagram representation of a turbo IB-DFE receiver.

When using channel coding data bits must be encoded and mapped into symbols prior to transmission. Turbo equalization in FD includes decoding/encoding and soft demap-

ping/mapping. The equalized samples at the output of the equalizer are demapped in order to provide LLRs for each coded bit. It follows a decoder to retrieve the data bits, which are mapped and encoded as the original data was at the transmitter. Thus, the feedback loop of the turbo IB-DFE provides improved soft estimations which lead to much better overall performance.

Considering the previous used example of a constellation QPSK, with symbols $\{\pm 1 \pm 1j\}$, soft mapping and demmaping is actually quite simple.

The complex log likelihood ratio for n^{th} time domain symbol of the transmitted block at the input of the channel decoder is defined as

$$\lambda_n = \lambda_n^I + j\lambda_n^Q, \tag{3.20}$$

where λ_n^I and λ_n^Q are associated to $Re\{s_n\}$ and $Im\{s_n\}$, respectively, where, the soft demmaper yields [34]

$$\lambda_n = \frac{4\tilde{s}_n}{\sigma_{CN}^2}, \tag{3.21}$$

with σ_{CN}^2 being the variance of the complex noise at the output of the equalizer. It is clear from the previous equation that the log likelihood is proportional to the equalizer soft output.

After decoding, an improved complex log likelihood ratio, $\eta_n^I + j\eta_n^Q$, is obtained, i.e. $|\eta_n| > |\lambda_n|$, which yields the equalizer soft output as

$$\tilde{s'}, n = \tanh\left(\frac{\eta_n^I}{2}\right) + j\tanh\left(\frac{\eta_n^Q}{2}\right), \tag{3.22}$$

and the steps of the soft IB-DFE on ρ computation described in the previous section, follow. By working on improved soft symbols estimation/better LLRs, a considerable improvement in performance is observed [29].

Notice that this analysis is done considering a SC-FDE modulation for sake of simplicity. Further, in the next chapter, a different analysis is done to fully grasp the experimental procedures. For now, the system description done in this chapter allows a basic understanding of the concept of IB-DFE receivers aiming to its application to the BWB-OFDM scheme.

4

BWB-OFDM with Frequency Domain Equalization

The transceiver scheme BWB-OFDM proposed in [3] [2] proved that its transmitted signals can have PSD as compact as filtered OFDM schemes, since it also employs smoother, non-rectangular, windows therefore, avoiding ACI and emphasizing an efficient bandwidth usage. Moreover, the BER performance is better than filtered and conventional OFDM schemes and even allows a PAPR reduction, allowing a smoother operating condition of power amplifiers. Nevertheless, the system lacks an improved receiver that can attain BER performances as close as the theoretical limit (*matched filter bound*).

The IB-DFE receiver, presented in chapter 3, is implemented and its BER performance is evaluated. Since simulation results show that BWB-OFDM transmissions with an IB-DFE receiver over time-dispersive channels are poorly performed, the basic characteristics of the wireless channel environment are reviewed. Furthermore, it is concluded that the BWB-OFDM with IB-DFE receiver could not deal with deep fades occurring in those environments which motivates the introducing of the new time-interleaved BWB-OFDM transceiver. The time-*interleaver* approach allows the receiver to recover corrupted data, thus showing considerable improvement towards the BWB-OFDM scheme. Also, the commitment between spectrum confinement and transmission rate as well as the PAPR level decrease is kept showing that the new time-*interleaved* transceiver has nothing but overall improvement towards the BWB-OFDM scheme. Finally, the employment of turbo IB-DFE receivers allows BER performances close to matched filter bound performance.

This new transceiver scheme is considered as a time-*interleaver* since the symbols are *interleaved* in time-domain creating replicas of its spectra. Those replicas are the key to deal with deep fading when considering transmission over time-dispersive channels.

4.1 BWB-OFDM with IB-DFE Receiver

This section proposes a BWB-OFDM receiver with IB-DFE implementation. Thus, the linear FDE at the receiver is replaced for a nonlinear FDE.

For sake of description simplicity consider the IB-DFE receiver, depicted in Fig. 4.1.

The equalization in the frequency domain of the BWB-OFDM received block, Y_k ($DFT_{Nx}\{y_n\}$), is performed by the IB-DFE. The output of this equalizer, at the i^{th} iteration, can be written as

$$\tilde{S}_k^{(i)} = F_k^{(i)} Y_k - B_k^{(i)} \hat{S}_k^{(i-1)}, \tag{4.1}$$

where $F_k^{(i)}$: $\{k = 0, 1, ..., N_x - 1\}$ are the feedforward coefficients and $B_k^{(i)}$: $\{k = 0, 1, ..., N_x - 1\}$ are the feedback coefficients. $\hat{S}_k^{(i-1)}$: $\{k = 0, 1, ..., N_x - 1\}$ denotes the *hard decision* of estimated symbols S_k from the previous iteration. In order to proceed to take the *hard decision* on S_k, there is some processing to perform. First $\tilde{S}_k$ is converted to time-domain, i.e. $\tilde{s}_n = IDFT_{Nx}\left\{\tilde{S}_k\right\}$ and has its ZP removed. Then, the resulting time-domain block

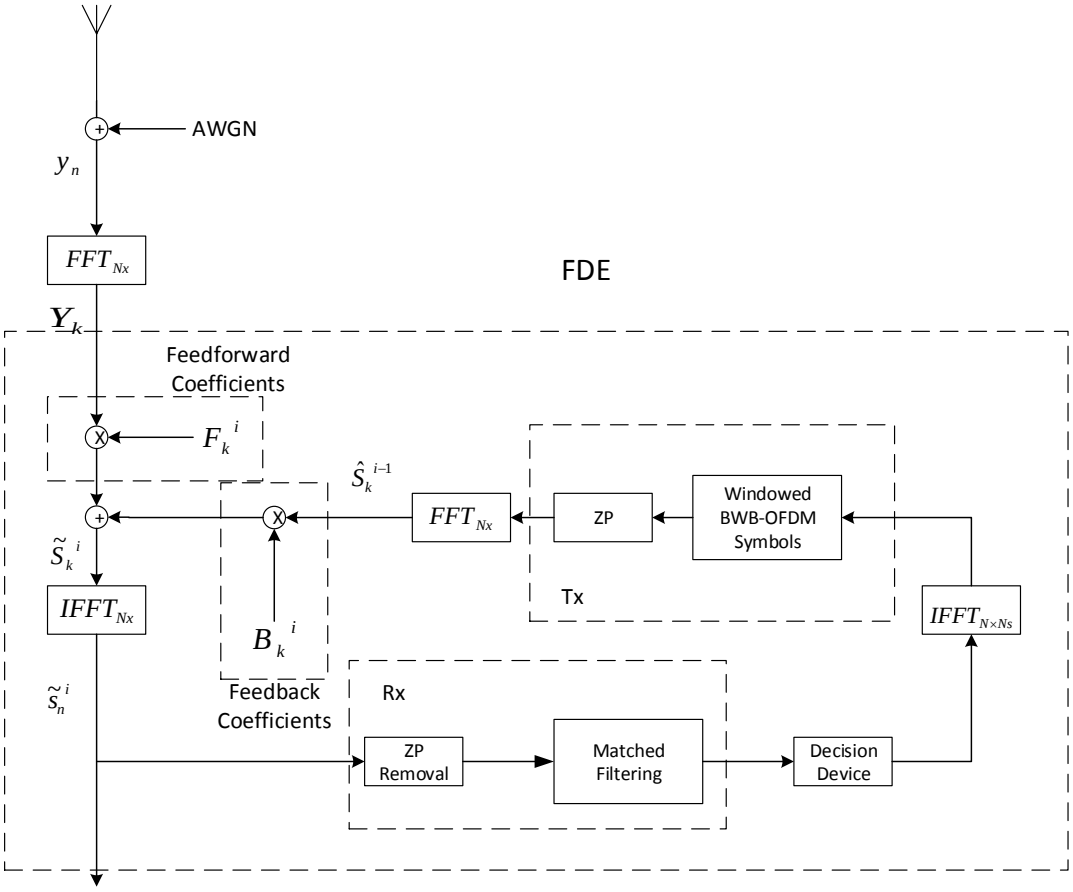

Figure 4.1: Diagram of BWB-OFDM with IB-DFE receiver.

proceeds to the typical BWB-OFDM receiver in order to estimate the original data, described by the *Matched Filtering* block [1]. In this, as described in section 2.2.3, the $\tilde{s}_n$ block is converted from serial to parallel and each symbol is extended up to $2N$ length by adding zeros at both ends in order to perform the windowing (*matched filtering*) followed by a conversion to frequency domain through a $(N_s \times 2N)$-sized FFT. The original data estimation is obtained by decimating the previous result followed by a parallel to serial conversion.

The *hard decision* is performed on the estimated data and converted to time-domain by the means of a $(N \times N_s)$-sized IFFT. Then, the *hard decision*, in time-domain, follows the same process as the original data at the transmitter, described by the *Windowed BWB-OFDM Symbols* block [2]. The block is converted from serial to parallel and proceeds to cyclic extension and windowing. It follows a parallel to serial conversion and the adding

[1] Regard Fig. 2.8 for *Matched Filtering* block-diagram.
[2] Regard Fig. 2.7 for *Windowed BWB-OFDM Symbols* block-diagram.

of the ZP.

The resulting frequency domain block, $\hat{S}_k$, yields the estimation of S_k. The system proceeds until the last iteration is performed.

Finally, the output of the IB-DFE, $\tilde{S}_k$, follows the same processing as $\tilde{S}_k^{(i)}$, at the i^{th} iteration. However, after the estimation of the original data, it proceeds to demmaping and, if channel coding is used, deinterleaving and decoding.

4.1.1 Simulation results

The following simulations were performed considering a BWB-OFDM transmission scheme with an IB-DFE receiver, through a dispersive channel. In both simulations it was considered $N = 64$ sub-carriers, and QPSK modulation under a Gray coding rule. Also, both use a BWB-OFDM symbol of length $N_x = 2048$ with $N_s = 21$ and a SRRC window with $\beta = 0.5$.

In Fig. 4.2, it is simulated the proposed system for a transmission with and without channel coding. When using channel coding, it is employed a (64,128) short low-density parity-check code (LDPC), and bit-interleaving is applied over sixteen consecutive coded words. For an uncoded transmission, the presented BER performance shows, clearly, that the IB-DFE shows no improvement as we increase the number of iterations, standing still at the same performance as a MMSE equalizer. For channel coding transmissions over a dispersive channel results are even poorer, with degradation in BER performance for each new iteration, showing that some error propagation throughout the feedback loop occurs.

4.1.2 Final Comments

Clearly, the results depicted in Fig. 4.2 show that the IB-DFE aplplied to original proposed BWB-OFDM scheme, cannot deal with transmissions over dispersive channels for which IB-DFE is particularly suited. Without channel coding, the successive iterations could not improve the BER performance showing poor ability to minimize the ISI and the interference due to past incorrect estimations, employed at the feedback loop. With channel coding, at the 2^{nd} iteration, the system, clearly, breaks down, worsening the BER performance and shows no sign of improvement in future iterations. The results are clear and show that nonlinear equalization cannot deal with deep fades in dispersive channels for the BWB-OFDM case.

So, the proposed BWB-OFDM scheme requires changes so that IB-DFE can outperform the linear equalizers, dealing with the occurrence of deep fades.

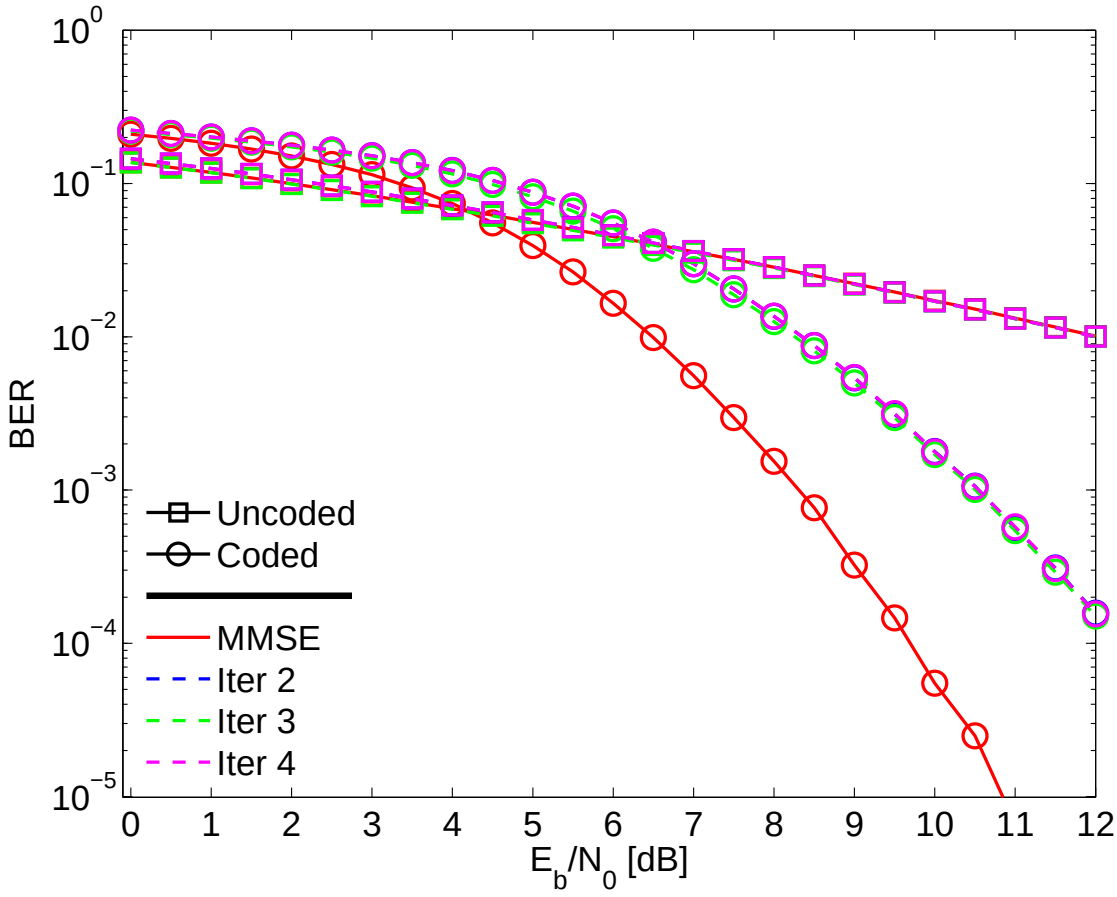

Figure 4.2: BER results for BWB-OFDM with IB-DFE receiver, coded and uncoded transmission, over dispersive channel.

4.2 Time Interleaver

The previous simulation results proved that the nonlinear equalizer implemented was unsuccessful. Although, in theory, the BWB-OFDM transceiver is analogous to a SC-FDE scheme from the receiver, the IB-DFE could not perform well. To understand the problem, one has to figure out how a dispersive fading channel affects signal transmission.

Throughout previous chapters it was often mentioned the problem of time-dispersion occurring in wireless channels. That occurrence is caused by the multipath propagation phenomenon that typical wireless environments exhibit, where the waves arrive at the receiver antenna from many directions with random amplitudes, frequencies and phases. The dispersion arises because the signal suffers many reflections when propagating through paths with different lengths, and, hence, reaching the receiver antenna with different time-delays.

A multipath channel can be modeled as a linear time-variant filter having the complex

low-pass impulse response [18]

$$h(t,\tau) = \sum_{n=1}^{N} C_n e^{j\phi_n(t)\delta(\tau-\tau_n)}, \tag{4.2}$$

where C_n, ϕ_n, and τ_n are the random amplitude, phase, and time delay, respectively, associated with the n^{th} propagation path, and N is the total number of arriving multipath components.

The constructive and destructive addition of waves combined with motion results in envelope fading, where the received envelope can vary significantly. Then, the main problem is due to deep fades that often occur.

BWB-OFDM Fading Issue

The main BWB-OFDM drawback is related to the deep fading issue. In order to describe it, consider the BWB-OFDM transmitter where the BWB-OFDM symbols, $s_{w,i}$, with $i = 1,...,N_s$ are packed together to form a mega block, s_B, see Fig. 4.3 . Recall from past sections that each BWB-OFDM symbol has a length of $N(1+\beta)$ and, for sake of simplicity, in the examples that follow and support the subsequent analysis we consider $N_s = 3$ and that the interval guard ZP is not added.

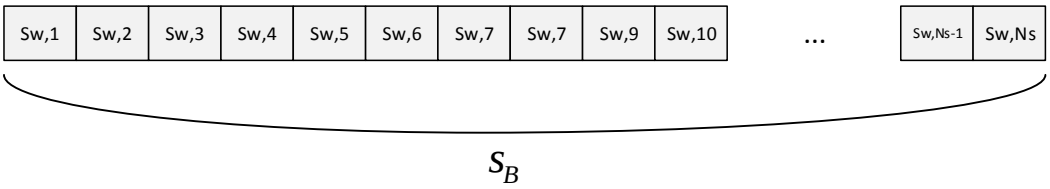

Figure 4.3: Time-domain transmitted block.

The effect that a wireless deep fading channel has on this current transmission scheme can be devastating. Considering a spectral analysis it is straightforward to show how the deep fading experienced by the transmitted signal is affected. The signal amplitude spectrum of the transmitted block consists on a superimpose of all N_s symbol spectra. For ease of reference, regard Fig. 4.4.

Consider the assumption previously made, were the transmitted block is the result of only three assembled symbols. The previous figure shows the signal spectrum amplitude of those three symbols. As mentioned, the superposition of those represented spectra yields the resulting signal amplitude spectrum. Now, consider that the channel has a deep fading region around a certain range of frequencies, as depicted in Fig. 4.4. The spectral

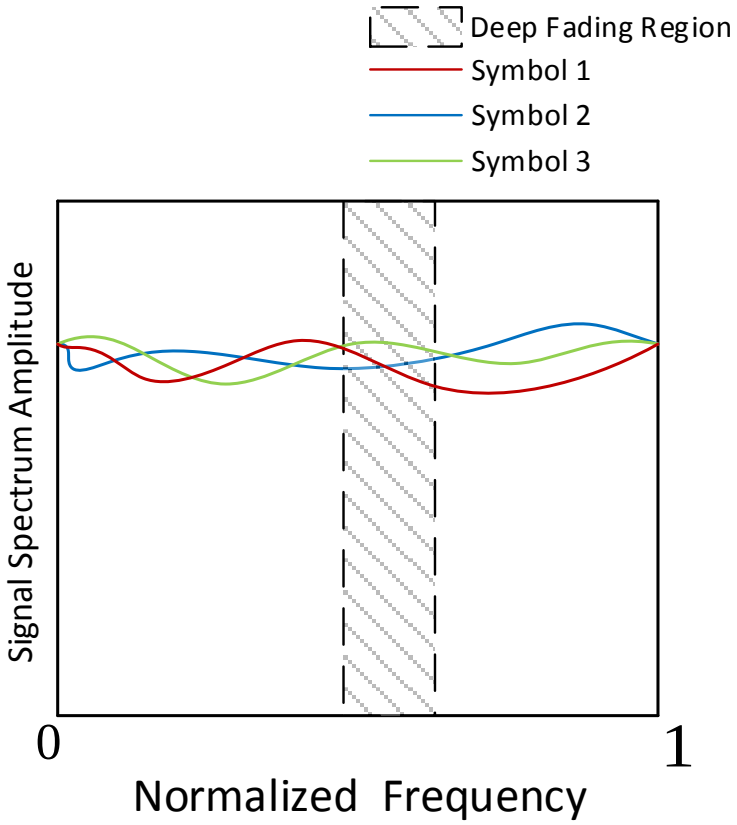

Figure 4.4: Signal spectrum amplitude of a BWB-OFDM transmitted block.

content inside that region will be completely destroyed, corrupting the data information of the three represented BWB-OFDM symbols. That corrupted data will hardly be recovered. Moreover, the previous simulation showed that the IB-DFE receiver could not recover that data and it even worsened the error propagation problem.

So, when a deep fade occurs, the data has such a high corruption level that the transmitted information will be lost. A possible solution to deal with deep fading occurrences lies on the possibility of having spare data containing the original information prior to corruption. The easiest way to preserve all data susceptible of being destroyed is to replicate the information throughout the assigned bandwidth.

The $s_{w,i}$ spectrum can be compressed and replicated by an expander system, shown in Fig. 4.5. Let $x[n]$ be the original sequence in discrete time-domain. An expanded sequence, $y_e[n]$, is obtained by introducing $L-1$ null samples between the original sequence samples and can be expressed as [35]

$$y_e[n] = \begin{cases} x[n/L] & , \quad n \; mod \; L = 0 \\ 0 & , \quad otherwise \end{cases} \tag{4.3}$$

Note that no information is lost by expanding the original sequence. The expanded

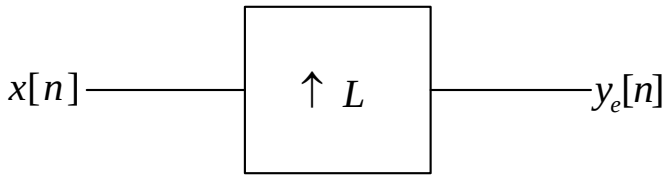

Figure 4.5: Expander system order L.

sequence has the same energy as the original, since only zeros are added. The expanded sequence spectrum presents $L-1$ compressed replicas of the original spectrum and can be expressed as

$$Y_e(e^{jw}) = X(e^{jwL}). \tag{4.4}$$

Let's now consider the i^{th} original BWB-OFDM symbol, $s_{w,i}$. By expanding each sequence $s_{w,i}$ individually by a N_s factor, the expanded BWB-OFDM symbol spectrum would present $N_s - 1$ compressed replicas of the original spectrum. When considering that all N_s symbols are perfectly aligned with the first symbol, i.e., discarding the delay of each one [3], the resulting expanded BWB-OFDM symbol can be written as

$$s^*_{e,i}[n] = \begin{cases} s^*_{w,i}[n/N_s] & , \quad n \; mod \; N_s = 0 \\ 0 & , \quad otherwise \end{cases} \tag{4.5}$$

for $n = 0, 1, ..., N_b - 1$, where $s^*_{w,i}$ is the i^{th} original BWB-OFDM symbol without delay and $N_b = N_s \times N(\beta + 1)$. The N_s expanded BWB-OFDM symbols are sketched in Fig. 4.6.

[3] We are considering the symbols at the output of the IFFT blocks before parallel-to-serial conversion and mega-block assembly, as shown in Fig. 2.7.

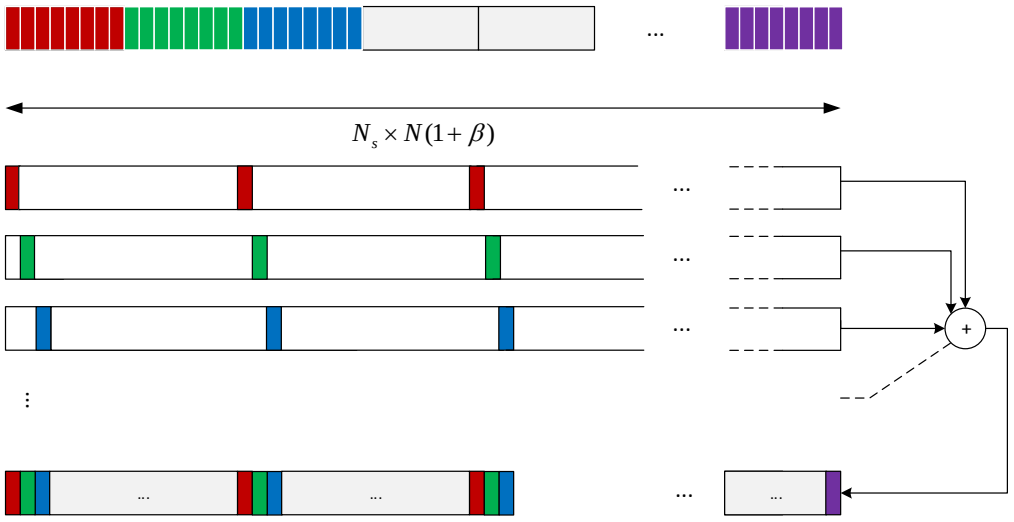

Figure 4.6: Sketch of the time-interleaved BWB-OFDM transmitted block.

Leveraging on the previous reasoning, we propose a new time-interleaved BWB-OFDM scheme. The new mega-block, results from a time-interleaving of the samples of symbols $s_{w,i}$, $i = 0, ..., N_s - 1$ can be written as

$$s_{Bi} = \sum_{i=0}^{N_s} s^*_{e,i}[n-i]. \tag{4.6}$$

The spectrum of the new time-interleaved block can be written as

$$S_{Bi}(e^{jw}) = \sum_{i=0}^{N_s} S^*_{e,i}(e^{jw})e^{-jwi}, \tag{4.7}$$

where $S^*_{e,i}(e^{jw}) = S^*_{w,i}(e^{jwN_s})$[4] is the spectrum of the i^{th} expanded BWB-OFDM symbol. We still have a superposition of the spectra of each individual symbols $s_{w,i}$, but now, due to the time expansion the spectra of each of these symbols is replicated in the frequency N_s times.

Fig. 4.7 presents the new spectra amplitude shape, corresponding to the example presented in Fig. 4.6. The spectral content inside the deep fading region is affected and that information is permanently lost. However, there are two more data backup replicated throughout the assigned bandwidth. Then, the corrupted data is not completely lost (just degraded), since it is still possible to recover it from the remaining unaffected regions that save up the same information.

Although it may seem counter-intuitive because the spectral information is a mess of superimposed spectra, the created diversity allows a solving problem to deep fading wireless channels.

[4] $S^*_{w,i}$ is the spectrum of the i^{th} original BWB-OFDM symbol without delay

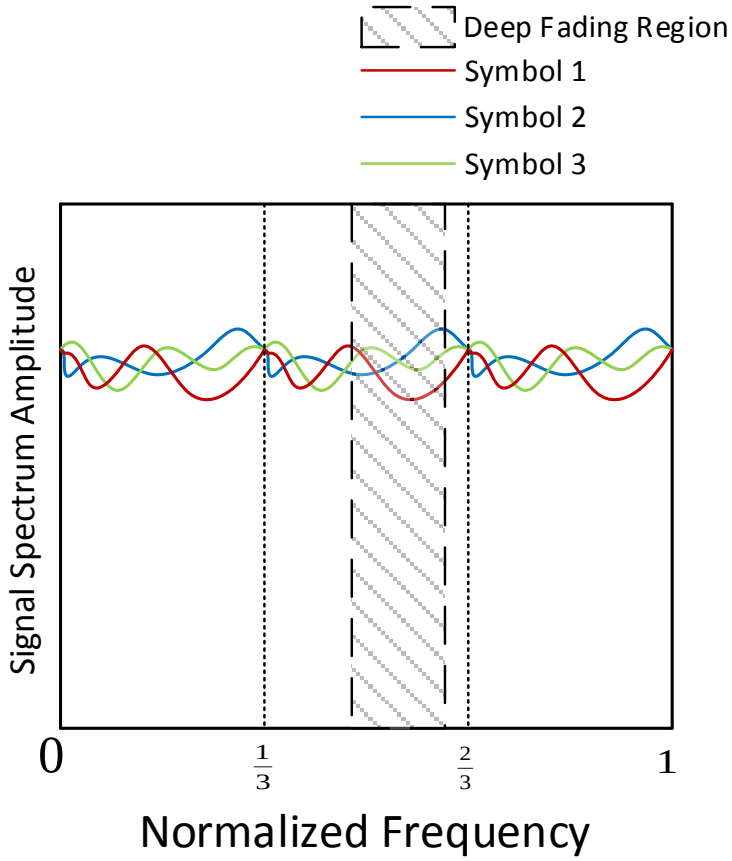

Figure 4.7: Signal spectrum amplitude of a time-interleaved BWB-OFDM transmitted block.

This new kind of time-interleaver will be implemented in a remodeled transceiver scheme in the subsequent sub-chapter.

4.3 Time Interleaved BWB-OFDM

4.3.1 Transmitter

The proposed time-interleaved BWB-OFDM transmitter is built on the BWB-OFDM transmitter, Fig. 4.8. Main transceiver differences refer to mega-block assembly using time-interleaving, and windowing to perform spectral shaping.

The modulated symbols, S_k: $\{k = 0, 1, ..., N-1\}$, at the k^{th} sub-carrier, are obtained from a direct mapping of a bit stream, with channel coding and bit interleaving applied, into a selected signal constellation. Employing bit-interleaving in transmissions over dis-

persive channels is really important because what it does is to spread eventual burst errors, that usually occur, allowing error correction codes to easily deal with the spread errors.

The symbol stream is separated into N low-rate sub-streams by an IFFT. Recall from eq. 2.25 that the complex envelope of a baseband OFDM symbol can be described in discrete time-domain as

$$s_n = s[n] = \sum_{k=0}^{N-1} S_k w[n] e^{j2\pi k \frac{n}{N}}. \tag{4.8}$$

For ease of signal processing, the time-interleaver is applied at this point. Each one of the OFDM symbols, $s_{n,i}$, where $i = 1,...,N_s$ are interleaved between each other, resulting in N_s interleaved symbols, $s_{int,i}$, where $i = 1,...,N_s$. Each interleaved symbol is the result of the following rule, see Fig. 4.6. The symbols $s_{int,i}$, where $i = 1,...,N_s$ are packed together to form a single block of N_s time-interleaved BWB-OFDM symbols.

Let $s_{Bint} = s_{Bint}[n]$, where $n = 0,1,...,(N \times N_s) - 1$, describe the interleaved BWB-OFDM mega-block. In order to keep the achieved spectrum, depicted in Fig. 2.6, there is the need to apply cyclic extension and windowing, resulting the mega-block, written in matrix form as

$$s_B = \begin{bmatrix} s_{Bint} & | & s_{Bint} \end{bmatrix}_{(1\times 2(N\times N_s))} \odot \mathbf{h}_{SRRC_{(1\times 2(N\times N_s))}}, \tag{4.9}$$

where the window $\mathbf{h}_{SRRC_{(1\times 2(N\times N_s))}}[n]$ is expressed by eq. 2.26. Note that windowing is now applied to the mega-block and not individually to each symbol component as in the original scheme.

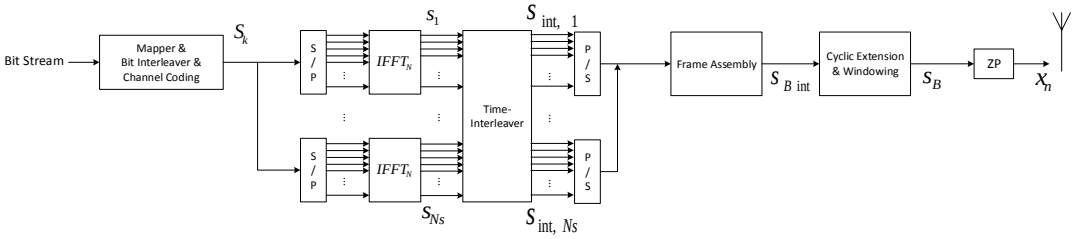

Figure 4.8: Diagram of time-interleaved BWB-OFDM transmitter.

The spectrum confinement follows the same improvement as the BWB-OFDM transmitter, increasing the number of samples per transmitted symbol to $N(1+\beta)$. To accommodate the multipath channel's propagation delay, a guard interval (ZP) is added at the end of the block. Then, the transmitted BWB-OFDM symbol can be written as

$$x_n = \begin{bmatrix} s_B & | & 0_{(1\times N_{zp})} \end{bmatrix}_{(1\times N_x)}, \tag{4.10}$$

where $0_{(1\times N_{zp})}$ represents a null vector of length N_{zp} and $N_x = N_s \times N(1+\beta) + N_{zp}$ is the total length of the transmitted block.

4.3.2 Receiver

The time-interleaved BWB-OFDM receiver is represented in Fig. 4.9. Its main role is to equalize the received signal, perform matched filtering, so ACI is rejected, and perform the time-deinterleaving and perform matched filtering, so ACI is rejected, before soft demodulation, bit-deinterleaving and channel decoding.

The received signal, y_n, with $n = 0, 1, ..., N_x - 1$, is converted to frequency domain by the means of a N_x-sized DFT, resulting in Y_k, with $k = 0, 1, ..., N_x - 1$. Considering that the chosen duration of the guard interval is larger than the duration of the channel impulse response, Y_k can be written as

$$Y_k = H_k X_k + \eta_k, \tag{4.11}$$

with $X_k = DFT\{x_n\}$, where DFT denotes the discrete Fourier transform, and H_k and N_k denote, at the k^{th} sub-carrier, the channel frequency response and the complex additive white Gaussian noise (AWGN) with variance $2\sigma_n^2 = E[|\eta_k|^2]$, respectively [2].

This is followed equalization, which can be performed with one of the previously addressed equalizers: MMSE, ZF or IB-DFE. In the analysis and the presented results that will follow, only the MMSE and IB-DFE equalizers will be considered only, since ZF has a poor performance in time dispersive channels as mentioned before.

The equalized signal, $\hat{X}_k$ with $k = 1, ..., N_x$, is converted to the time-domain by the means of a N_x-sized IDFT and has its ZP removed. The resulting block has the same SRRC window applied in order to perform matched filtering, by extending the block with zeros at both ends until it gets a length of $2N_B$. Then, it follows the same rule applied at the transmitter in order to apply the time-deinterleaver. The resulting block is then split into symbols $\hat{x}_{n,i}$: $i = 1, .., N_s$ with $n = 0, 1, ..., N(1+\beta) - 1$.

The estimated symbols $\hat{x}_{w,i}$ are converted to frequency-domain by the means of a N-sized FFT and converted from parallel-to-serial which yields the estimate of the original data, S_k.

Note that at this point, the noise variance can be obtain, approximately, by

$$\sigma_\eta^2 = \frac{\varepsilon_S}{N_B} \sum_{l=0}^{N_B-1} \frac{1}{1+\gamma|H_l|^2}, \tag{4.12}$$

where ε_S is the variance of the original modulated symbols [5] and $N_B = N_s \times N(1+\beta)$.

Next, the estimates, $\hat{S}_{k,i}$, are demodulated. For QPSK constellations, the LLRs are given by

$$\Lambda(b_0) = log\left(\frac{P_r\left(b_0 = 0|\hat{S}_{k,i}[l]\right)}{P_r\left(b_0 = 1|\hat{S}_{k,i}[l]\right)}\right) = -\frac{4Re\left[\hat{S}_{k,i}[l]\right]}{\sigma_\eta^2} \tag{4.13}$$

$$\Lambda(b_1) = log\left(\frac{P_r\left(b_1 = 0|\hat{S}_{k,i}[l]\right)}{P_r\left(b_1 = 1|\hat{S}_{k,i}[l]\right)}\right) = -\frac{4Im\left[\hat{S}_{k,i}[l]\right]}{\sigma_\eta^2} \tag{4.14}$$

At last, to estimate the original binary sequence $\hat{b}$, it is applied deinterleaving and channel decoding.

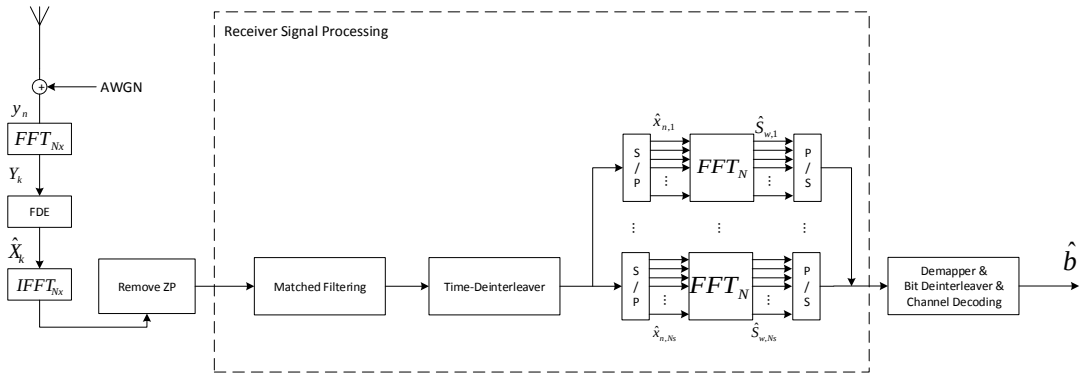

Figure 4.9: Diagram of time-interleaved BWB-OFDM receiver.

4.3.3 BWB-OFDM versus time-interleaved BWB-OFDM

This section compares the new proposed scheme with the BWB-OFDM scheme presented in chapter 2. The evaluation of the performance of the new scheme allows to obtain numerical results that shows how the new time-interleaving idea allows the system to endure severely dispersive channels. The comparison between the two transceiver schemes is performed establishing the equalizer with a MMSE criteria. Then, the equalized received signal is obtained by 2.33. Also, both systems employ QPSK modulation under a Gray coding rule and $N = 64$ sub-carriers. When channel coding is applied, it is employed by a $(64, 128)$ LDPC code [5], and bit-interleaving is applied over sixteen consecutive coded words. The same window is applied with a roll-off of $\beta = 0.5$, yielding a symbol with length $N_x = 2048$ with $N_s = 21$. The BER performance comparison is evaluated for both schemes over a severe time-dispersive channel.

Simulation Results

The following simulations compare the BER performance between BWB-OFDM and time-interleaved BWB-OFDM schemes, with and without channel coding, over a dispersive channel. When channel coding is not used the time-interleaved BWB-OFDM scheme presents a much better performance than the BWB-OFDM scheme. This evolution is due to the multiple replicas which save up most part of the corrupted data. This performance

[5] This short LDPC code was chosen due to its match with the $N = 64$ sub-carriers

also allows the new scheme to outperform the old one by 1dB, approximately, when channel coding is used.

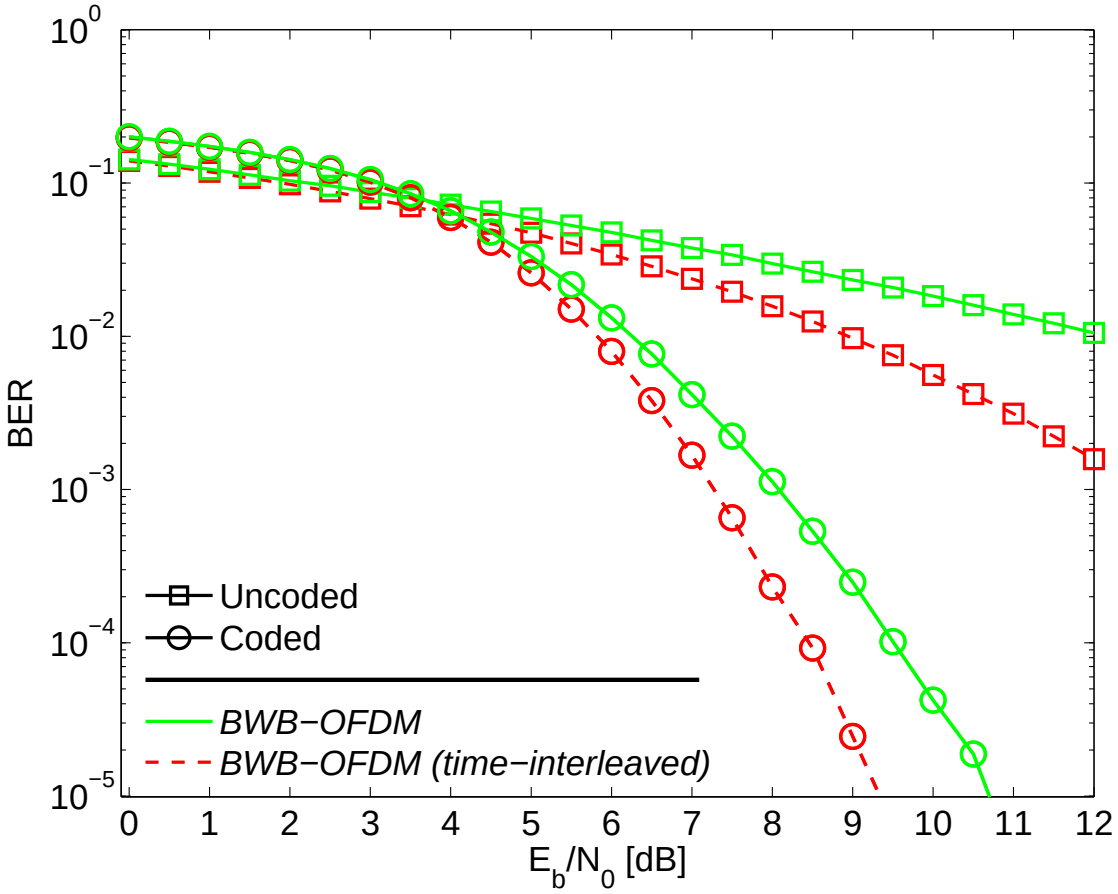

Figure 4.10: BER results for BWB-OFDM and time-interleaved BWB-OFDM, both coded and uncoded transmissions, over a dispersive channel.

4.3.4 Time-Interleaved BWB-OFDM with IB-DFE

This section proposes a time-interleaved BWB-OFDM receiver with IB-DFE implementation. Mainly, the FDE in Fig. 4.9 is replaced by the IB-DFE system depicted in Fig. 4.11. The equalization in the frequency domain of the received block, Y_k, is performed by the IB-DFE, same as it was done in 4.1, where the output of the equalizer, at the i^{th} iteration, can be written as

$$\tilde{S}_k^{(i)} = F_k^{(i)} Y_k - B_k^{(i)} \hat{S}_k^{(i-1)}, \tag{4.15}$$

where $F_k^{(i)}$: $\{k = 0, 1, ..., N_x - 1\}$ are the feedforward coefficients and $B_k^{(i)}$: $\{k = 0, 1, ..., N_x - 1\}$ are the feedback coefficients. $\hat{S}_k^{(i-1)}$: $\{k = 0, 1, ..., N_x - 1\}$ denotes the *hard decision* of S_k from the previous iteration.

The *hard decision*, $\hat{S}_k$ is performed by the decision device after the conversion of $\tilde{S}_k$ to time-domain by the means of a N_x-sized IFFT, which yields $\tilde{s}_n$, and some receiver processing necessary to estimate. The process requires a complete unformatting of the received mega-block as previously defined. Note that the feedforward branch is similar to a MMSE equalizer in the absence of the feedback loop.

The resulting estimate is converted back to frequency-domain by the means of a N_x-sized FFT, yielding the *hard decision*, $\hat{S}_k$. The IB-DFE proceeds its iterative method until the last iteration is performed.

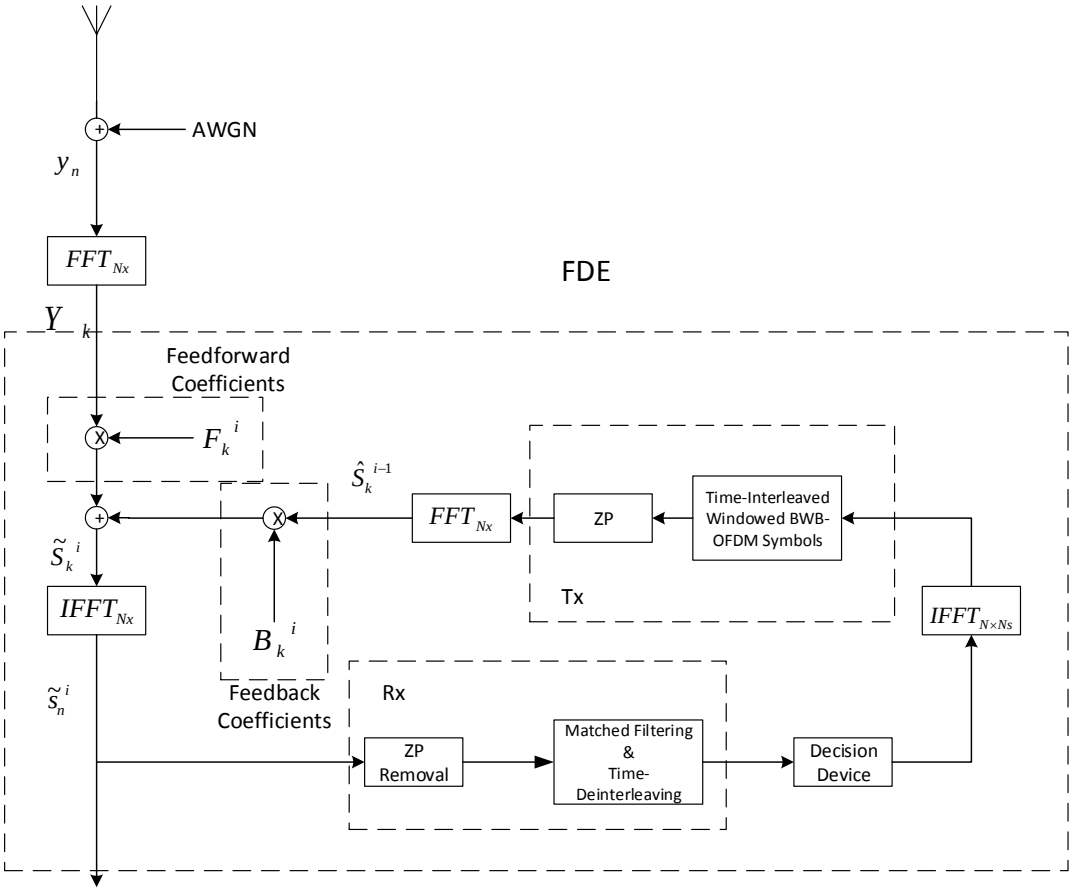

Figure 4.11: Diagram of time-interleaved BWB-OFDM with IB-DFE receiver.

Simulation Results

The following simulations were performed considering a *time-interleaved* BWB-OFDM transmission scheme with an IB-DFE receiver, through a dispersive channel. Also, the previously simulated BWB-OFDM transmission, over a dispersive channel, with channel

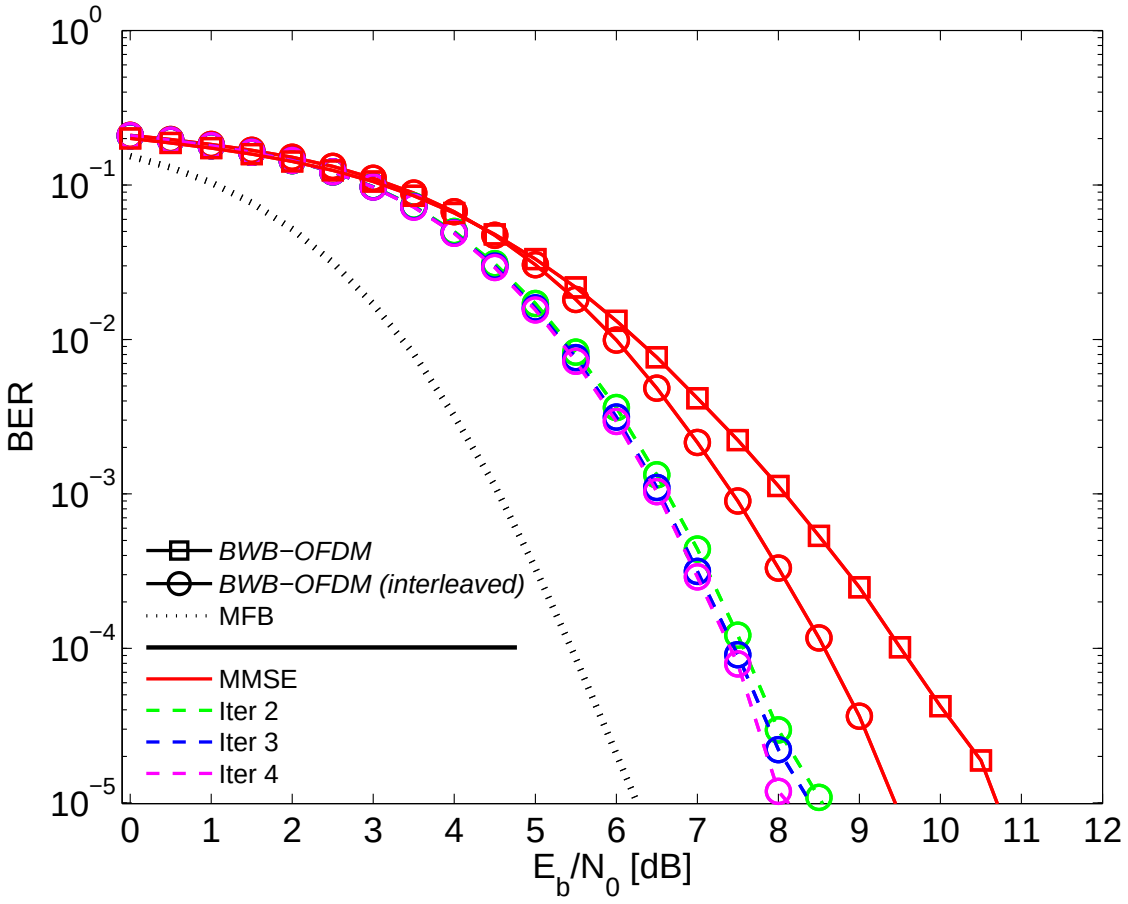

Figure 4.12: BER results for BWB-OFDM with MMSE criteria and time-interleaved BWB-OFDM with IB-DFE receiver, over dispersive channel.

coding for the MMSE criteria is also used for comparison purposes. In both simulations it was considered $N = 64$ sub-carriers, and QPSK modulation under a Gray coding rule. Also, both use a BWB-OFDM symbol of length $N_x = 2048$ with $N_s = 21$ and a SRRC window with $\beta = 0.5$. Channel coding is employed by using a $(64, 128)$ LDPC short code, and bit-interleaving is applied over sixteen consecutive coded words. The results are depicted in Fig. 4.12. , showing the BER performance of the BWB-OFDM transmission under MMSE criteria and the first 4 iterations of the time-interleaved BWB-OFDM transmission with an IB-DFE receiver. The MFB BER performance is also depicted, see Fig. 4.12.

The simulation result, see Fig. 4.12, shows that the IB-DFE receiver applied to the time-interleaved BWB-OFDM transmission could deal with the occurring deep fades with small error propagation and shows some evolution from iteration to iteration. The proposed time-interleaved BWB-OFDM with an IB-DFE receiver has almost 3dB improvement over the BWB-OFDM with MMSE criteria scheme and it is just less than 2dB from the theoretical limit (MFB). Note also, that the bulk of this gain, can be obtained with just

two iterations of the IB-DFE algorithm, showing its fast convergence.

4.3.5 Time-Interleaved BWB-OFDM with Turbo IB-DFE

This section proposes a time-interleaved BWB-OFDM receiver with Turbo IB-DFE implementation aiming for a performance closer to theoretical limit (MFB). Essentially, the FDE in Fig. 4.9 is replaced by the Turbo IB-DFE system depicted in Fig. 4.13, as done in the previous configuration.

When employing Turbo IB-DFE, the system expects an improvement in BER performance. The main difference lies on the feedback loop, which employs decoding and deinterleaving on the process to estimate data. A better estimation will improve the likeness between data and its respective estimate, thus yielding a better correlation coefficient, which eases the removal of possible interference due to previous imperfect estimations.

The employment of coding/decoding and bit-interleaving/bit-deinterleaving in the feedback loop is pretty important since the it helps to reduce the errors caused by occurring deep fades.

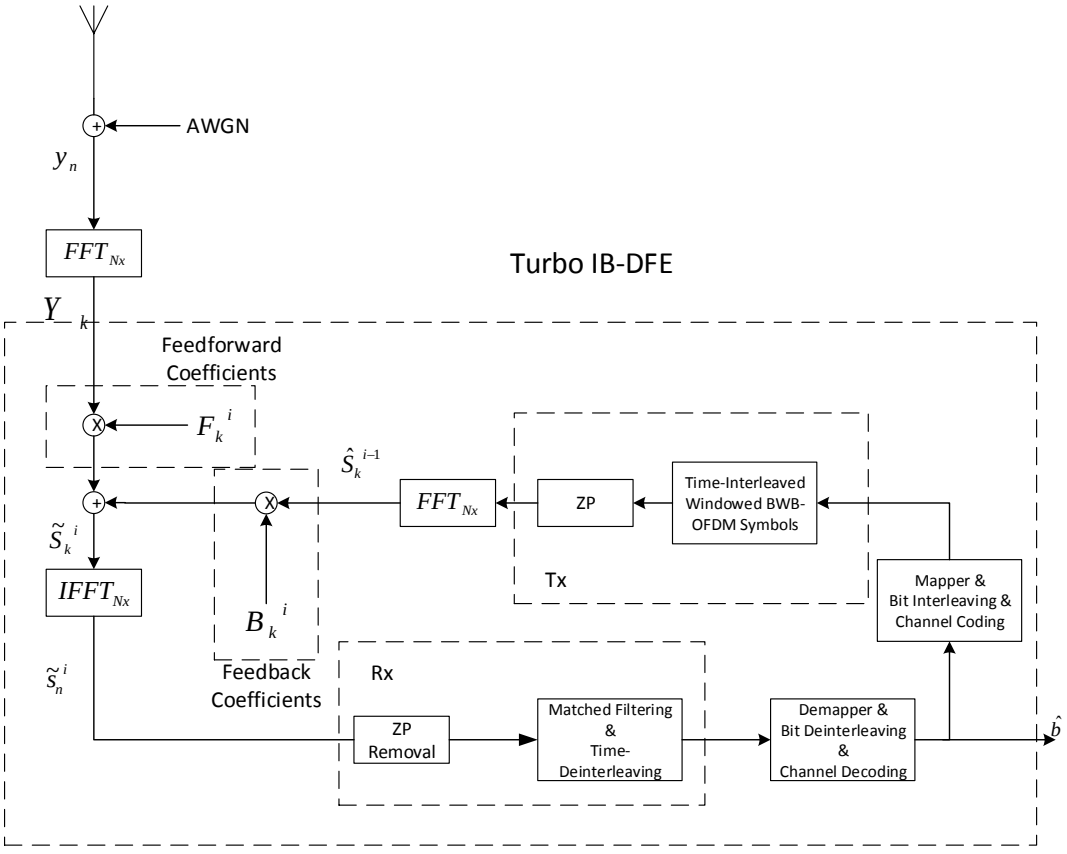

Figure 4.13: Diagram of time-interleaved BWB-OFDM with Turbo IB-DFE receiver.

Simulation Results

The following simulations were performed considering a time-interleaved BWB-OFDM transmission scheme with a Turbo IB-DFE receiver, through a dispersive channel. In order to perform decoding/deinterleaving to each received block, there were made some necessary changes to the system configuration. In both simulations it was considered $N = 64$ sub-carriers, and QPSK modulation under a Gray coding rule. Also, both use a BWB-OFDM symbol of length $N_x = 4096$ with $N_s = 42$ and a SRRC window with $\beta = 0.5$. Channel coding is employed by using a $(64, 128)$ LDPC short code, and bit-interleaving is applied over twenty-one consecutive coded words. Note that the block

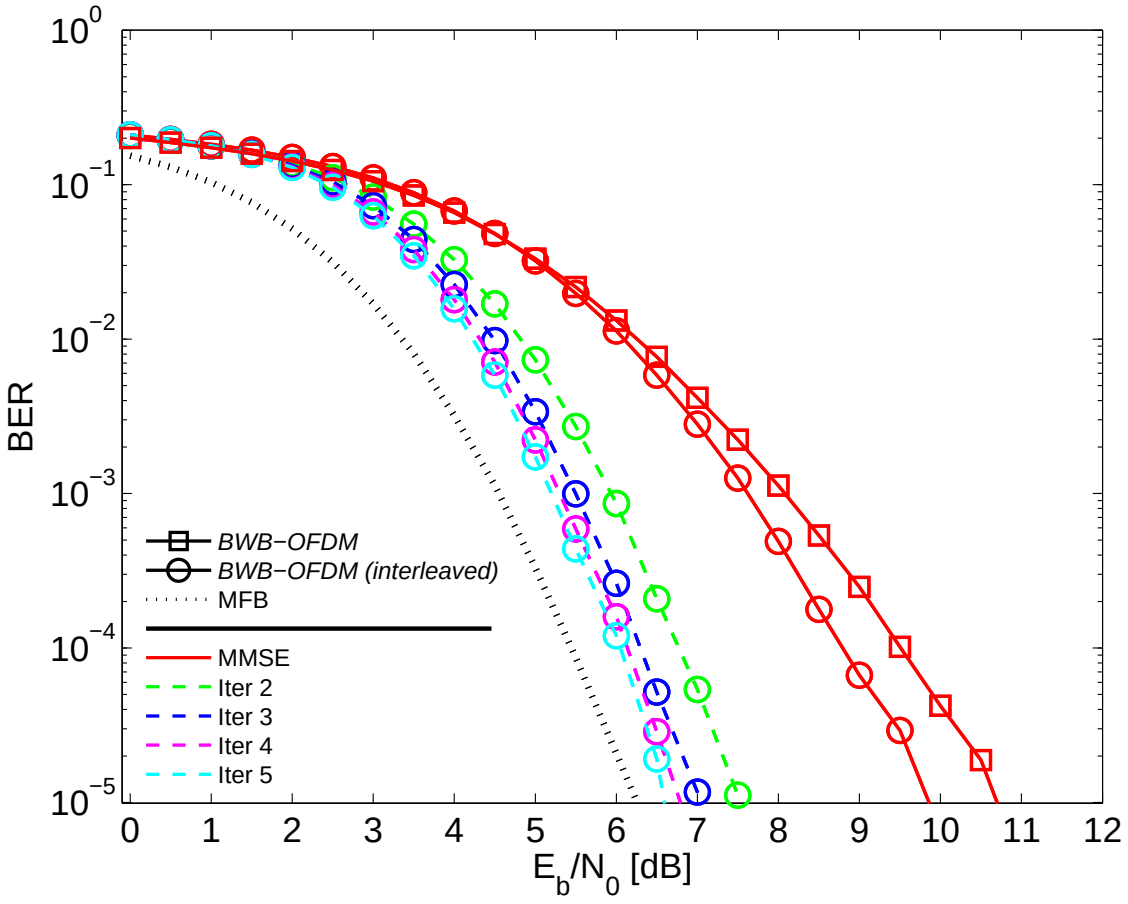

Figure 4.14: BER results for BWB-OFDM with MMSE criteria and time-interleaved BWB-OFDM with Turbo IB-DFE receiver, over dispersive channel.

length it was doubled from past simulations. This was necessary due to the fact that before, the bit-interleaver was applied to two consecutive blocks and with this new configuration, the bit-interleaver is only applied to a single block, allowing the turbo IB-DFE to employ coding/decoding and bit-interleaving/bit-deinterleaving in its feedback loop. In

another words, to perform bit-deinterleaving in the turbo loop $N \times N_s$ has to the multiple of length(LDPC)/$\log_2(M) = 64$.

The results are depicted in Fig. 4.14, showing the BER performance of the BWB-OFDM transmission under MMSE criteria and the first 4 iterations of the time-interleaved BWB-OFDM transmission with a Turbo IB-DFE receiver. The MFB BER performance is also depicted.

The expect BER performance improvement is confirmed by the result of the carried out simulation, see Fig. 4.14. The last iteration of the turbo IB-DFE is only less than 0.5dB from the theoretical limit (MFB). This shows that the time-interleaver at the transmitter united with the encoder/interleaver at the feedback loop grant a substantial BER performance improvement.

4.3.6 PAPR

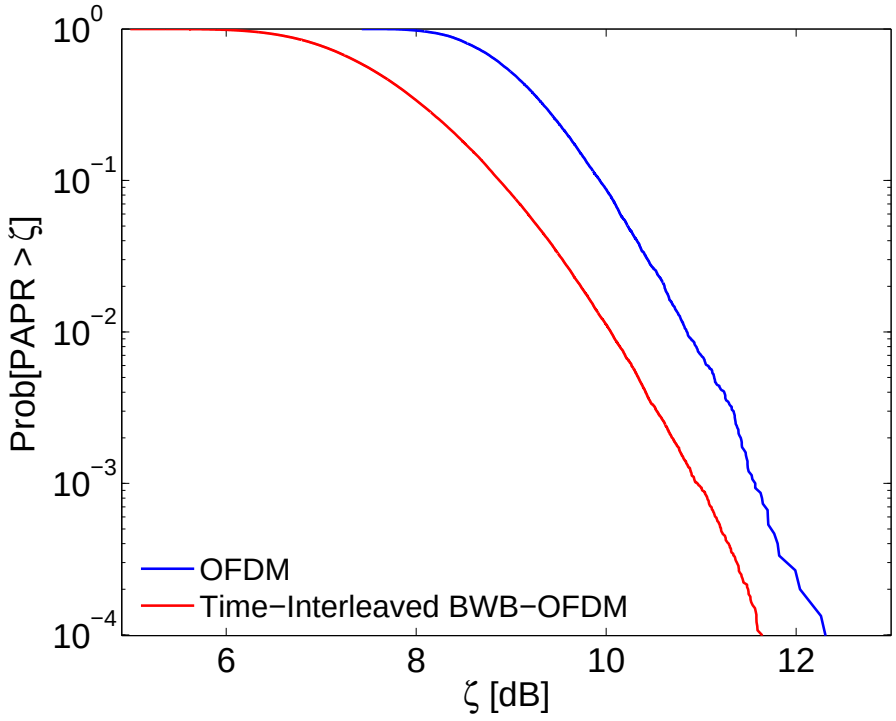

Figure 4.15: CCDF for PAPR for CP-OFDM and time-interleaved BWB-OFDM.

This section ends discussion with a PAPR analysis of the new proposed system. PAPR is a symbol measurement parameter and so the comparison between typical OFDM schemes and the new time-interleaved BWB-OFDM scheme is done between the time-interleaved BWB-OFDM block with $N = 64$ and $N_s = 28$ and a OFDM symbol with $N = 2048$.

The new scheme keeps the same gain, about 0.5dB, towards the typical OFDM system, see Fig. 4.15. This gain allows a more efficient operation of the power amplifier since the distance between the maximum peak signal and the signal average is lower, relaxing the power amplifier conditions for *back-off*.

5

Conclusions

This thesis addressed the potential of a new proposed transceiver scheme, *time-interleaved* BWB-OFDM, combined with an IB-DFE receiver. The motivation of this new system arose from the attempt on combining IB-DFE with the recent proposed BWB-OFDM transceiver scheme. BWB-OFDM can be seen as a hybrid transmission scheme and a flexible alternative to other block based transmission techniques, such as OFDM and SC-FDE, allowing for considerable trade-off gains in power and spectral efficiency, and as so having a potential of interest taken. However, the attempt on combining IB-DFE with it, revealed the main drawback of this transceiver scheme. When transmitting over severe time-dispersive channels, IB-DFE and BWB-OFDM are useless combined.

The focus turned to time-dispersive channels and its deep fade experience. To overcome this issue, a possible solution was proposed. The time-interleaving of the transmitted symbols, resulting in a simple remodel of the BWB-OFDM scheme, turned out to yield considerable results when compared to BWB-OFDM with MMSE receiver. This indicator pointed towards the development of a better receiver, namely, the previously attempted, IB-DFE receiver. The BER performance was greatly improved when IB-DFE and time-interleaved BWB-OFDM were combined. Furthermore, the improvement was increased when turbo IB-DFE was applied, reaching a very good BER performance only about 0.5dB from the theoretical limit (MFB).

Since the spectral confinement and PAPR levels achieved by the BWB-OFDM schemes were preserved, the time-interleaved BWB-OFDM scheme proved to be a reliable alternative to previously mentioned tecnhiques, achieving a better overall performance.

Ultimately, we come to conclusion that the applied time-interleaver is of utmost importance when dealing with severe time-dispersive channels, proving to be a major asset to the BWB-OFDM transceiver scheme with IB-DFE receiver.

5.1 Future Work

Although great results were achieved with the proposal of the *time-interleaved* BWB-OFDM transceiver scheme, the system is still pretty limited. Since channel coding is applied using short LDPC codes, the system only presents good BER performance in relatively high SNR environments. Moreover, several assumptions were made. The channel was considered perfectly estimated and the synchronization critical issue was not considered which does not offer a realistic evaluation. However, the time-interleaver approach has potential and should be explored considering channel estimation, different coding and perhaps a multi input multi output (MIMO) implementation. Also it would be of interest to explore the possible different architecture configurations.

Bibliography

[1] K. Fazel and S. Kaiser, *Front Matter*. Wiley Online Library, 1997.

[2] J. Nunes, "Sistema ofdm multi-símbolo: Uma abordagem multiportadora eficiente," Master's thesis, Universidade de Coimbra, 2014.

[3] J. Nunes, P. Bento, M. Gomes, R. Dinis, and V. Silva, "Block-windowed burst ofdm: a high-efficiency multicarrier technique," *Electronics Letters*, vol. 50, no. 23, pp. 1757–1759, 2014.

[4] T.-D. Chiueh and P.-Y. Tsai, *OFDM baseband receiver design for wireless communications*. John Wiley & Sons, 2008.

[5] Y.-P. Lin, S.-M. Phoong, and P. Vaidyanathan, *Filter bank transceivers for OFDM and DMT systems*. Cambridge University Press, 2010.

[6] R. Prasad, *OFDM for wireless communications systems*. Artech House, 2004.

[7] S. H. Han and J. H. Lee, "An overview of peak-to-average power ratio reduction techniques for multicarrier transmission," *Wireless Communications, IEEE*, vol. 12, no. 2, pp. 56–65, April 2005.

[8] Y. Rahmatallah and S. Mohan, "Peak-to-average power ratio reduction in ofdm systems: A survey and taxonomy," *Communications Surveys Tutorials, IEEE*, vol. 15, no. 4, pp. 1567–1592, Fourth 2013.

[9] J. G. Proakis, "Digital communications. 1995," *McGraw-Hill, New York*.

[10] W. Zou and Y. Wu, "Cofdm: an overview," *Broadcasting, IEEE Transactions on*, vol. 41, no. 1, pp. 1–8, Mar 1995.

[11] N. Weste and D. Skellern, "Vlsi for ofdm," *Communications Magazine, IEEE*, vol. 36, no. 10, pp. 127–131, Oct 1998.

[12] N. Marchetti, M. I. Rahman, S. Kumar, and R. Prasad, "Ofdm: Principles and challenges," in *New Directions in Wireless Communications Research*. Springer, 2009, pp. 29–62.

[13] U. S. Jha and R. Prasad, *OFDM towards fixed and mobile broadband wireless access*. Artech House, Inc., 2007.

[14] Q. Shi, Y. Fang, and M. Wang, "A novel ici self-cancellation scheme for ofdm systems," in *Wireless Communications, Networking and Mobile Computing, 2009. WiCom '09. 5th International Conference on*, Sept 2009, pp. 1–4.

[15] L. Yu, B. Rao, L. Milstein, and J. Proakis, "Reducing out-of-band radiation of ofdm-based cognitive radios," in *Signal Processing Advances in Wireless Communications (SPAWC), 2010 IEEE Eleventh International Workshop on*, June 2010, pp. 1–5.

[16] W. Fisher, "Digital video and audio broadcasting technology," 2008.

[17] A. Item, "3rd generation partnership project," *Korea*, vol. 10, p. 13, 2000.

[18] Y. G. Li and G. L. Stuber, *Orthogonal frequency division multiplexing for wireless communications*. Springer Science & Business Media, 2006.

[19] R. v. Nee and R. Prasad, *OFDM for wireless multimedia communications*. Artech House, Inc., 2000.

[20] T. Hwang, C. Yang, G. Wu, S. Li, and G. Li, "Ofdm and its wireless applications: A survey," *Vehicular Technology, IEEE Transactions on*, vol. 58, no. 4, pp. 1673–1694, May 2009.

[21] R. Dinis and A. Gusmao, "On the performance evaluation of ofdm transmission using clipping techniques," in *Vehicular Technology Conference, 1999. VTC 1999-Fall. IEEE VTS 50th*, vol. 5. IEEE, 1999, pp. 2923–2928.

[22] L. J. Cimini Jr and N. R. Sollenberger, "Peak-to-average power ratio reduction of an ofdm signal using partial transmit sequences," *Communications Letters, IEEE*, vol. 4, no. 3, pp. 86–88, 2000.

[23] T. Jiang and Y. Wu, "An overview: peak-to-average power ratio reduction techniques for ofdm signals," *IEEE transactions on broadcasting*, vol. 54, no. 2, p. 257, 2008.

[24] B. Farhang-Boroujeny, "Ofdm versus filter bank multicarrier," *Signal Processing Magazine, IEEE*, vol. 28, no. 3, pp. 92–112, 2011.

[25] R. Dinis, J. Conceição, N. Esteves *et al.*, "Comparison of two modulation choices for broadband wireless communications," in *Vehicular Technology Conference Proceedings, 2000. VTC 2000-Spring Tokyo. 2000 IEEE 51st*, vol. 2. IEEE, 2000, pp. 1300–1305.

[26] D. Falconer, S. L. Ariyavisitakul, A. Benyamin-Seeyar, and B. Eidson, "Frequency domain equalization for single-carrier broadband wireless systems," *Communications Magazine, IEEE*, vol. 40, no. 4, pp. 58–66, 2002.

[27] J. G. Proakis, *Intersymbol Interference in Digital Communication Systems*. Wiley Online Library, 2001.

[28] F. Coelho, R. Dinis, N. Souto, and P. Montezuma, "On the impact of multipath propagation and diversity in performance of iterative block decision feedback equalizers," in *Wireless and Mobile Computing, Networking and Communications (WiMob), 2010 IEEE 6th International Conference on*. IEEE, 2010, pp. 246–251.

[29] N. Benvenuto, R. Dinis, D. Falconer, and S. Tomasin, "Single carrier modulation with nonlinear frequency domain equalization: an idea whose time has come—again," *Proceedings of the IEEE*, vol. 98, no. 1, pp. 69–96, 2010.

[30] R. Dinis, A. Gusmao, and N. Esteves, "On broadband block transmission over strongly frequency-selective fading channels," 2003.

[31] R. Dinis, P. Silva, and A. Gusmao, "Ib-dfe receivers with space diversity for cp-assisted ds-cdma and mc-cdma systems," *European Transactions on Telecommunications*, vol. 18, no. 7, pp. 791–802, 2007.

[32] N. Benvenuto and S. Tomasin, "Iterative design and detection of a dfe in the frequency domain," *Communications, IEEE Transactions on*, vol. 53, no. 11, pp. 1867–1875, 2005.

[33] R. Dinis, P. Montezuma, N. Souto, and J. Silva, "Iterative frequency-domain equalization for general constellations," in *Sarnoff Symposium, 2010 IEEE*. IEEE, 2010, pp. 1–5.

[34] G. Cherubini and N. Benvenuto, "Algorithms for communications systems and their applications," 2003.

[35] T. Saramäki and R. Bregovic, "Multirate systems and filter banks," *Multirate systems: design and applications*, vol. 2, pp. 27–85, 2001.